SCATTERING FROM DIELECTRIC-COVERED PERIODIC SCREENS OF SMALL RECTANGULAR APERTURES

Quirino Balzano, et al

Raytheon Company

Prepared for:

Air Force Cambridge Research Laboratories

March 1974

UNCLASSIFIED

SECURITY CLASSIFICATION OF THIS PAGE (When Data Entered)

AD 782 027

REPORT DOCUMENTATION PAGE		READ INSTRUCTIONS BEFORE COMPLETING FORM
1. REPORT NUMBER AFCRL-TR-74-0173	2. GOVT ACCESSION NO.	3. RECIPIENT'S CATALOG NUMBER
4. TITLE (and Subtitle) Scattering from Dielectric-Covered Periodic Screens of Small Rectangular Apertures		5. TYPE OF REPORT & PERIOD COVERED Scientific Report No. 2 6. PERFORMING ORG. REPORT NUMBER BR-7997
7. AUTHOR(s) Quirino Balzano Lawrence R. Lewis Jerome F. Lezgay		8. CONTRACT OR GRANT NUMBER(s) F19628-72-C-0202
9. PERFORMING ORGANIZATION NAME AND ADDRESS Raytheon Company Missile Systems Division Bedford, Massachusetts 01730		10. PROGRAM ELEMENT, PROJECT, TASK AREA & WORK UNIT NUMBERS 62702F, 4600-11-01 674600
11. CONTROLLING OFFICE NAME AND ADDRESS Air Force Cambridge Research Labs (LZ) L. G. Hanscom Field Bedford, Massachusetts 01730		12. REPORT DATE March 1974 13. NUMBER OF PAGES 53
14. MONITORING AGENCY NAME & ADDRESS(if different from Controlling Office)		15. SECURITY CLASS. (of this report) Unclassified 15a. DECLASSIFICATION/DOWNGRADING SCHEDULE

16. DISTRIBUTION STATEMENT (of this Report)

A - Approved for public release; distribution unlimited.

17. DISTRIBUTION STATEMENT (of the abstract entered in Block 20, if different from Report)

18. SUPPLEMENTARY NOTES

Tech, Other

19. KEY WORDS (Continue on reverse side if necessary and identify by block number)

Self-Complementary Screens
Periodic Screens of Rectangular Apertures
Relative Convergence
Capacitive Screens
Scattering

20. ABSTRACT (Continue on reverse side if necessary and identify by block number)

A study of the use of perforated screens as potential radome structures has been conducted. The self-complementary nature of these screens suggests their application for broadbanding or harmonic filters, while aiding the structural integrity of the radome. The adjustment of radome parameters is important to the control of wide angle radiation from radome-covered conformal arrays.

DD FORM 1 JAN 73 1473 EDITION OF 1 NOV 65 IS OBSOLETE

UNCLASSIFIED

SECURITY CLASSIFICATION OF THIS PAGE (When Data Entered)

20. ABSTRACT (Cont.)

The analysis of plane wave scattering by infinitesimally thin periodic screens of rectangular apertures is developed and applied to the scattering by dielectric slab-covered self-complementary screens.

For small aperture self-complementary screens ($s/\lambda < 0.21$), it is found that the reflection coefficient magnitude and phase for normally incident plane waves are characteristic of a shunt susceptance of small, nearly constant capacitance. In this frequency range ($s/\lambda < 0.21$), the deviation from the static capacitance (evaluated as $s/\lambda \rightarrow 0$) is small. Using the static capacitance value, computed reflection coefficients for dielectric slab-covered self-complementary screens are shown to be in excellent agreement with experiment over a three octave frequency band.

ACKNOWLEDGMENT

The authors gratefully acknowledge the substantial help given by Mr. C. J. Hunt in the experimental program.

TABLE OF CONTENTS

LIST OF ILLUSTRATIONS

LIST OF ILLUSTRATIONS (Cont.)

1. INTRODUCTION AND SUMMARY

This report describes the results of an investigation of the use of self-complementary screens as broadband devices to plane wave incidence. Two antennas are said to be complementary if the radiated electric and magnetic fields of one are the same as the magnetic and electric fields radiated by the other. One of the more familiar pairs is the slot and dipole. There are also complementary surfaces (screens), where the complement of a screen containing metal ($\sigma = \infty$) and a perfect magnetic conducting material ($\mu = \infty$) is a screen with the materials interchanged. A self-complementary screen is one where the interchange of metallic and magnetic conducting surfaces reproduce the identical configuration and possesses the properties of a superimposed pair of complementary screens. The qualification that a perfect magnetic conductor be used is eliminated if these regions are replaced by a nonconducting material (i. e., free space, perfect dielectric) provided that the structure has translational and rotational symmetry. A self-complementary screen which has these properties is shown in Figure 1.

During late 1969 and early 1970, Raytheon conducted an experimental investigation of plane wave scattering from thin-dielectric slab covered self-complementary screens. The results of these early investigations showed that for arrays of small apertures, $s/\lambda \leq 0.1$, the dielectric-slab covered self-complementary screen was highly transmissive over an octave frequency band. A maximum transmission loss of 1.5 dB was observed over the band for small aperture screens ($s/\lambda \cong 0.2$) with thin-dielectric slab covering ($h/\lambda \leq 0.048$).

The results of the current study confirmed that the screen of small apertures is highly transmissive; however, when used in combination with dielectrics suitable for radomes at microwave frequencies, the self-complementary screen will not enhance the bandwidth. More significantly, for increasing frequency ($s/\lambda \gtrsim 0.1$ to $s/\lambda \lesssim 0.21$), the reflection characteristics of the uncovered screen are such that a constant shunt capacitive susceptance is

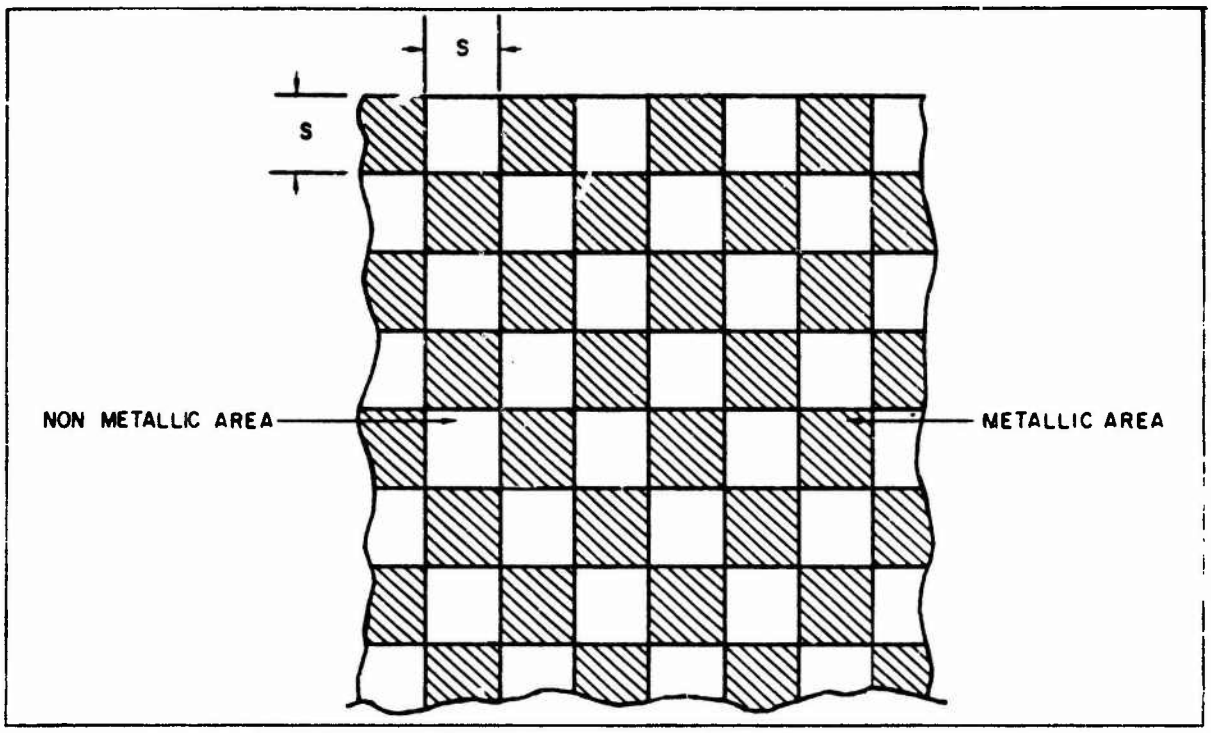

Figure 1 - Self-Complementary Screen

realized. The constant capacitive element characteristic suggests the use of self-complementary screens as:

1) Low pass filters or filter sections;
2) Dispersionless capacitive microwave circuit elements;
3) Harmonic filters in waveguides or integrated to radomes, and
4) Matching devices in waveguides.

In recent years, the problem of scattering by thin periodic conducting screens of rectangular apertures[1, 2] and the complementary problem of scattering by periodic arrays of thin-rectangular plates[3] have been given considerable attention due to the passband and stopband characteristics of such devices for apertures at resonance. In 1961, Kieburtz and Ishimaru[1] used a variational technique to evaluate scattering by a periodically apertured screen into higher order diffraction lobes. The success of variational techniques depends on the proper choice of a trial function for the aperture field distribution, and in particular, becomes quite tedious and involved for off-broadside incidence. In 1967, Ott, Kouyoumjiam, and Peters[3] used the

multiple scattering method of Twersky[4] to evaluate scattering by a two-dimensional array of thin-narrow plates. This technique involves determining the N coefficients of the series representation for the surface current by solving the integral equation at exactly N points on a single plate. While Ott, et al. obtained excellent agreement with experiments, the solution is very sensitive to the location of the N points at which the integral equation is satisfied.

The technique in the present work is similar in many respects to that employed by Chen[2]. By virtue of the screen periodicity, the unknown fields on either side of the screen are expanded in a Floquet series. Enforcing boundary conditions for tangential field components in the plane of the screen, results in an integral equation for the unknown electric field in the apertures. The aperture electric field is expanded in a set of orthonormal mode functions and matching is carried out by a method of moments solution. This results in N equations for the N unknown modal voltages of the aperture. Knowledge of these voltages permits solution for the entire field.

The principal departure of the present analysis from that reported by Chen[2] is in the manipulation of the tangential magnetic field continuity equation to obtain an integral equation with a strongly convergent form of the kernel. Symmetry arguments are used to show that for principal plane incidence, periodic screens of rectangular apertures will not depolarize the fundamental scattered fields. The approximation is then made that the coefficient of each harmonic in the expansion of the zero magnetic field component is individually set to zero. This approximation results in rapidly convergent forms for the unknown field amplitudes. While no quantitative measure of the error in this approximation has been determined, the resultant formulation gives excellent agreement with experimental results for the range $0.02 < s/\lambda < 0.7$, as well as with the earlier computations of Kieburtz and Ishimaru for plane wave scattering by a square lattice screen of square apertures over the range $0.25 \leq s/\lambda \leq 1.0$.

In Section 2, a rigorous solution is obtained for scattering from uncovered screens. Particular attention is given to the convergence aspects of the numerical solution and the similarity to the relative convergence of numerical solutions found for a large class of iris diaphragm solutions[5, 6]. An equivalent network, in the form of a shunt capacitance, is shown to be a valid

representation of the screen discontinuity. The performance characteristics of the slab covered screen are then determined via the equivalent circuit representation.

In Section 3, measured reflection coefficient data over multi-octave bandwidths is presented for several dielectric slab covered screens. Comparisons with the corresponding numerical calculations shows excellent agreement.

A time dependence of $e^{j\omega t}$ has been assumed throughout.

2. ANALYSIS OF DIELECTRIC SLAB COVERED INFINITE PERIODIC SCREENS OF RECTANGULAR APERTURES

2.1 Field Matching in the Plane of the Screen

A plane wave is assumed incident from $z < 0$ at some angle, (θ_o, ϕ_o), on an infinitely thin, conducting periodic screen of rectangular apertures, as shown in Figure 2, where $\underline{s}_1$ and $\underline{s}_2$ are the basis vectors characterizing the unit cell of the periodic structure and $|\underline{s}_1 \times \underline{s}_2|$ is the cell area, c. The spacial variation of the fields in the transverse plane on either side of the screen have the form[7]

$$\psi_{pq}(\underline{s}) = \frac{1}{\sqrt{c}} \exp(-j\underline{u}_{pq} \cdot \underline{s}) \tag{1}$$

where $\underline{s}$ is the position vector within any cell given by

$$\underline{s} = x\hat{x} + y\hat{y}$$

and $\underline{u}_{pq}$ is the transverse wave vector defined as,

$$\begin{aligned} \underline{u}_{pq} &= \underline{u}_o + p\underline{t}_1 + q\underline{t}_2 \\ &= u_{pq}\hat{x} + v_{pq}\hat{y} \end{aligned} \tag{2}$$

The set of functions $\psi_{pq}(\underline{s})$ is complete and orthonormal over the unit cell. The indices p and q extend over all integers from $-\infty$ to ∞. The vectors, $\underline{t}_1$ and $\underline{t}_2$, reciprocal to the basis $\underline{s}_1$, $\underline{s}_2$ are determined by the relationships[8]

$$\underline{t}_i \cdot \underline{s}_k = 2\pi\delta_{ik} \tag{3}$$

$\underline{u}_o$ is the transverse wave vector which indicates the direction of the incident plane wave. Specifically

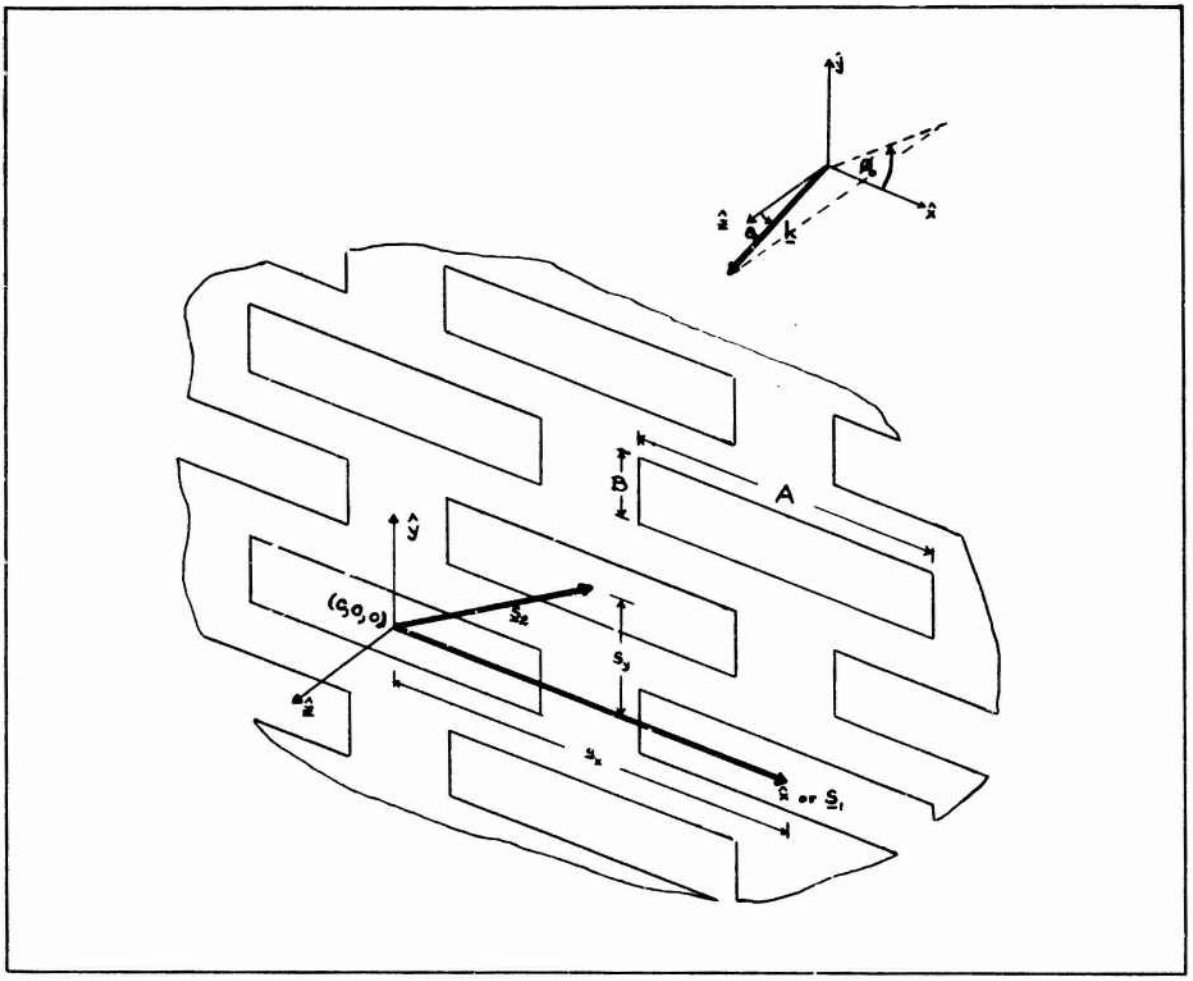

Figure 2 - Periodic Screen of Rectangular Apertures

$$\underline{u}_o = u_o\hat{x} + v_o\hat{y}$$

where

$$u_o = k \sin\theta_o \cos\phi_o$$

$$v_o = k \sin\theta_o \sin\phi_o$$

$$k = 2\pi/\lambda$$

From the wave equation and the radiation condition, the wave number in the positive z direction, w, is given by

$$w_{pq} = \sqrt{(k^2 - u_{pq}^2 - v_{pq}^2)} \tag{4}$$

where the negative root is taken for arguments less than zero.

The tangential electric field in the plane of the screen may then be expressed by the following bidimensional Floquet series*:

$$\underline{E}_t(\underline{s}) = \sum_{pq} \underline{A}_{t_{pq}} \psi_{pq}(\underline{s}) \tag{5}$$

The expansion (5) is valid over the entire unit cell. The transverse field coefficients, $\underline{A}_{t_{pq}}$, are vector functions which may be separated for convenience as,

$$\underline{A}_{t_{pq}} = A_{x_{pq}} \hat{x} + A_{y_{pq}} \hat{y}$$

Over the aperture in the cell, the tangential electric fields satisfy

$$\underline{E}_t^i(\underline{s}) + \underline{E}_t^r(\underline{s}) = \underline{E}_t^t(\underline{s}) \tag{6}$$

where the superscripts denote incident, reflected, and transmitted. Over the remainder of the cell, at z = 0, both sides of equation (6) are zero. Using equation (5) in the tangential electric field continuity equation, extended over

*To simplify the notation, the double summation $\sum_{p=-\infty}^{\infty} \sum_{q=-\infty}^{\infty}$ will be represented by $\sum_{pq}$.

the cell, and projecting the fields on the orthonormal functions $\psi_{pq}(\underline{s})$ the following relationships are obtained for the transverse electric field modal coefficients:

$$\underline{A}^{i}_{t_o} + \underline{A}^{r}_{t_o} = \underline{A}^{t}_{t_o}, \quad p = q = 0$$

and (7)*

$$\underline{A}^{r}_{t_{pq}} = \underline{A}^{t}_{t_{pq}}, \quad \text{all pq except } p = q = 0$$

Similar relations between the normal electric field coefficients follow from the plane wave definitions:

$$A^{i}_{z_o} - A^{r}_{z_o} = A^{t}_{z_o},$$

and (8)

$$-A^{r}_{z_{pq}} = A^{t}_{z_{pq}} \quad \text{all p, q except } p = q = 0.$$

The tangential magnetic field is continuous only over the aperture and is related to an unknown surface current over the remainder of the cell. The tangential magnetic field continuity equation valid in the aperture only is,

*The labeling of subscript '0', denotes p = q = 0, the dominant space harmonic.

$$\frac{1}{k\eta}\left\{\left[v_o A^i_{z_o} - w_o A^i_{y_o}\right]\hat{x} + \left[w_o A^i_{x_o} - u_o A^i_{z_o}\right]\hat{y}\right\}\psi_o(\underline{s})$$

$$+ \frac{1}{k\eta}\sum_{pq}\psi_{pq}(\underline{s})\left\{\left[v_{pq}A^r_{z_{pq}} + w_{pq}A^r_{y_{pq}}\right]\hat{x} - \left[w_{pq}A^r_{x_{pq}} + u_{pq}A^r_{z_{pq}}\right]\hat{y}\right\} =$$

$$\frac{1}{k\eta}\sum_{pq}\psi_{pq}(\underline{s})\left\{\left[v_{pq}A^t_{z_{pq}} - w_{pq}A^t_{y_{pq}}\right]\hat{x} + \left[w_{pq}A^t_{x_{pq}} - u_{pq}A^t_{z_{pq}}\right]\hat{y}\right\} \qquad (9)$$

By substituting equations (7) and (8) into equation (9) and rearranging the resultant expression a pair of scalar equations for the magnetic field continuity can be written as,

$$\frac{1}{k\eta}\psi_o(\underline{s})\left[\frac{v_o u_o}{w_o}\left(A^t_{x_o} - A^i_{x_o}\right) + \frac{k^2 - u_o^2}{w_o}\left(A^t_{y_o} - A^i_{y_o}\right)\right] =$$

$$j\frac{1}{k\eta}\sum_{p,q\neq o}\left[-\frac{v_{pq}u_{pq}}{|w_{pq}|}A^t_{x_{pq}} + \frac{u_{pq}^2 - k^2}{|w_{pq}|}A^t_{y_{pq}}\right]\psi_{pq}(\underline{s}) \qquad (10a)$$

$$\frac{1}{k\eta}\psi_o(\underline{s})\left[\frac{k^2 - v_o^2}{w_o}\left(A^t_{x_o} - A^i_{x_o}\right) + \frac{v_o u_o}{w_o}\left(A^t_{y_o} - A^i_{y_o}\right)\right] =$$

$$j\frac{1}{k\eta}\sum_{p,q\neq o}\left[\frac{v_{pq}^2 - k^2}{|w_{pq}|}A^t_{x_{pq}} - \frac{v_{pq}u_{pq}}{|w_{pq}|}A^t_{y_{pq}}\right]\psi_{pq}(\underline{s}) \qquad (10b)$$

where it is assumed only the zero harmonic is propagating.

The problem is now specialized to the case of principal plane incidence. In addition, linearly polarized excitation in $\hat{y}$ is assumed. The solution for the orthogonal excitation, (in $\hat{x}$) is analogous, and arbitrarily polarized excitation (i.e., skew linear, circular, elliptical) follows via superposition.

From the symmetries in periodic screens of identical rectangular apertures, as well as the specialized excitation, there will be no depolarization of the fundamental (propagating) scattered fields. Thus, on the left hand side (LHS) of equations (10) the A_{x_o} terms are zero. Moreover, for principal plane incidence either u_o or v_o is zero, hence the product term $u_o v_o$ is always zero. Equation (10b) becomes,

$$\frac{1}{k\eta} \sum_{pq \neq 0} \left[\frac{v_{pq}^2 - k^2}{|w_{pq}|} A^t_{x_{pq}} - \frac{u_{pq} v_{pq}}{|w_{pq}|} A^t_{y_{pq}} \right] \psi_{pq}(\underline{s}) = 0 \qquad (11)$$

in the aperture. As an approximation, the coefficients of the functions $\psi_{pq}(\underline{s})$ are individually set to zero. The motivation for this approximation is the highly convergent form of the resulting kernel in the integral equation. Moreover, the excellent agreement with experimental results for the self-complementry screen indicates that the higher order mode coupling, which is ignored by this approximation, is small. It follows from the approximation that,

$$A^t_{x_{pq}} \equiv \frac{-u_{pq} v_{pq}}{w_{pq}^2 + u_{pq}^2} A^t_{y_{pq}} \quad , \quad pq \neq 0 \qquad (12)$$

Substituting equation (12) into equation (10a) results in,

$$\psi_o(\underline{s}) \frac{k^2 - u_o^2}{w_o} A^i_{y_o} = \frac{1}{k\eta} \sum_{pq} \frac{k^2 w_{pq}}{w_{pq}^2 + u_{pq}^2} A^t_{y_{pq}} \psi_{pq}(\underline{s}) \qquad (13)$$

Of particular interest in equation (13) are the coefficients,

$$\frac{w_{pq}}{w_{pq}^2 + u_{pq}^2}$$

which are decreasing for increasing p and q. This is a considerable improvement over equations (10), which are essentially divergent. Equation (13) is now transformed into a set of matrix equations for the unknown aperture field.

Let the electric field distribution in the plane of the screen be

$$\begin{aligned} \underline{E}_t(\underline{s}) &= \sum_{m=1}^{\infty} V_m \underline{e}_m(\underline{s}) \quad \text{in the aperture} \\ &= 0 \qquad\qquad\qquad\quad \text{over the remainder of the cell} \end{aligned} \tag{14}$$

where the V_m are the unknown voltage amplitudes of the orthonormal aperture mode functions $\underline{e}_m(\underline{s})$. Enforcing the electric field continuity in the plane of the screen yields,

$$\sum_{m=1}^{\infty} V_m \underline{e}_m(\underline{s}) = \sum_{pq} \underline{A}_{t_{pq}} \psi_{pq}(\underline{s}) \text{ over the cell.} \tag{15}$$

Taking inner products of both sides of equation (15) with the set of functions $\psi_{rs}(\underline{s})$ results in expressions for the amplitude of the space modes in terms of the unknown aperture voltages. In particular, for the y components of the electric field:

$$A^t_{y_o} = \sum_{m=1}^{\infty} V_m \mathcal{E}_{y_{o,m}} \tag{16a}$$

and

$$A^t_{y_{rs}} = \sum_{m=1}^{\infty} V_m \mathcal{E}_{y_{rs,m}} \tag{16b}$$

where

$$\mathcal{E}_{y_{rs,m}} = 2\pi \int_{cell} \psi^*_{rs} e_{ym} \, dA \tag{17}$$

with the asterisk denoting complex conjugate.

Substituting equations (16) into (13) results in a magnetic field continuity equation in terms of the unknown aperture voltage amplitudes, V_m. Truncating the sums in the resulting expressions, and projecting both sides of the equation on the set of functions $\underline{e}_n(\underline{s})$, ($n = 1, \ldots, N$), results in a system of N linear equation in N unknown voltages, given as

$$\frac{1}{k\eta} \frac{k^2 w_o}{w_o^2 + u_o^2} A^i_{y_o} \mathcal{E}^*_{y_{o,u}} =$$

$$\frac{1}{k\eta} \frac{2\pi}{\sqrt{c}} \sum_{m=1}^{N} V_m \sum_{pq} \frac{k^2 w_{pq}}{w_{pq}^2 + u_{pq}^2} \mathcal{E}^*_{y_{pq,m}} \mathcal{E}_{y_{pq,n}} \quad n=1, 2 \ldots, N \tag{18}$$

The set of vector waveguide mode functions are a suitable choice for the aperture functions $\underline{e}_i$. For this particular set of functions, the coupling coefficients $\mathcal{E}$ have a convergent property which enhances the convergence of the term $k^2 w_{pq}/(w_{pq}^2 + u_{pq}^2)$. In particular, while not monotonic functions of p and q with respect to $p = q = 0$, the $\mathcal{E}$'s exhibit a monotonic decrease as p and q recede from a particular p' and q' in any direction, where p' and q' are related to the mode number. The expressions for the mode functions for rectangular apertures and the coupling coefficients, $\mathcal{E}$, are given in Appendix 3 of Reference (7).

It is instructive at this point to expand equation (18) for broadside incidence ($u_o = v_o = 0$) on the self-complementary screen using the explicit expressions for the coupling coefficients, $\mathcal{E}$, of the $TE_{n,o}$ modes where n is odd. Equation (18) becomes,

$$-A^{i}_{y_o}\frac{1}{n} = \frac{2}{\pi}\sum_{m=1}^{N} V_m \left\{ \frac{1}{mn} \right.$$

$$- j\frac{1}{k}\sum_{pq\neq o} \frac{|w_{pq}|}{1-(2q-p)^2(\lambda/2s)^2} \frac{nm\cos^2(p\frac{\pi}{2})}{(n^2-p^2)(m^2-p^2)} \qquad (19)$$

$$\left. \cdot \frac{\sin^2\left[(2q-p)\frac{\pi}{2}\right]}{\left[(2q-p)\frac{\pi}{2}\right]^2} \right\} \qquad n,m = 1,3,5,\ldots,N$$

For sufficiently small s/λ, ($s/\lambda \gtrsim 0.4$), the principal contributions occur for $p = n = m$. The significance of this is brought out in Subsection 2.2 where the convergence properties of the solution are discussed.

2.2 Remarks on the Method of Solution and its Consequences

The form of solution, equation (18), has a strong resemblance to that obtained for single interface waveguide array problem. Namely, that one can identify the multiplier

$$\frac{1}{\eta}\frac{kw_{pq}}{w_{pq}^2 + u_{pq}^2}$$

as an admittance term; specifically, the E-type modal admittance.[9] The choice of excitation is also an E-type mode; however, the nature of the approximation in the solution maintains coupling only to higher order E-type modes. This directly follows from equation (12). It is speculated that rapidly convergent forms of solutions will arise for similar screen, or diaphragm, problems using the type mode sets as the modal bases, in contrast to E or H modes.

The convergence properties for the solution set (18) are most simply presented for broadside incidence, for which it is convenient to consider only the $TE_{n,o}$ modes, where n is odd. For a triangular lattice, the coupling coefficients, $\mathcal{E}_{y_{pq,n}}$ have the dependence

$$\mathcal{E}_{y_{pq,n}} \propto \frac{n \cos\left[p\frac{\pi}{2}\left(\frac{2A}{s_x}\right)\right]}{n^2 - p^2\left(\frac{2A}{s_x}\right)^2}$$

where s_x is the x lattice dimensions and A is the x-dimension of the aperture. For the self-complementary screen, $s_x = 2A$, and this dependence reduces to

$$\mathcal{E}_{y_{pq,n}} \propto \frac{n \cos\left(p\frac{\pi}{2}\right)}{n^2 - p^2}$$

The maximum coupling between aperture and space modes will then occur for

$$|p| \approx n\, s_x/2A \tag{20}$$

Terms which do not satisfy approximation (20) will fall off at an approximate rate of $1/n$ or n/p^2. Namely, when the periodicity of the space harmonic is that of the aperture function in the corresponding plane, one of the N primary contributions to the sum in equation (18) is obtained. Furthermore, if P, the highest order space harmonic in the x direction and N, the highest order aperture mode number, are such that $P \approx Ns_x/2A$ is not true, then either:

1) P is too large and there is an insufficient number of aperture modes to approximate (match) the Pth space harmonic; or
2) N is too large and there is an insufficient number of space harmonics to match the Nth aperture mode.

A proper truncation of the modal sets must then be such that

$$P \approx Ns_x/2A \tag{21}$$

The $TE_{n,o}$ modes do not satisfy the edge condition in the E-plane. However, if ar appropriate modification of the mode functions is made, such that they retain their orthonormal characteristics over the aperture and individually satisfy the E-plane edge condition, there is virtually no change in the resultant reflection and transmission coefficients. A set of orthogonal functions that satisfy the edge condition are[1]

$$e_{y_n}(\underline{s}) \propto \sin\left(\frac{n\pi x}{A} - \frac{n\pi}{2}\right)\left[1 - (2y/B)^2\right]^{1/2} \qquad n = 1,2,\ldots$$

where A and B are the H and E-plane aperture dimensions, respectively; and $-A/2 \leq x \leq A/2$ and $-B/2 \leq y \leq B/2$. Then $\mathcal{E}_{y_{pq,n}}$ of $e_{y_n}(\underline{s})$ will be similar to the coupling coefficients obtained with the TE_{no} modes with $\sin(Bv_{pq}/2)/(Bv_{pq}/2)$ (see Appendix 3 of Reference 7) replaced by $J_1(Bv_{pq}/2)/(Bv_{pq}/2)$.

For $v_{pq} = 0$, the terms are identical, and for $v_{pq} \neq 0$ the Bessel function term decays slightly faster. For the self-complementary screen with small spacing ($s/\lambda \lesssim 0.21$) there is virtually no difference.

2.3 Numerical Examples

In this subsection, numerical examples are given for plane wave reflection by periodic screens of rectangular apertures. The discussion is limited to principal plane incidence, and the frequency regime is such that only one external propagating mode is present. Two geometries are considered: the self-complementary screen; and the square grid of square apertures studied by Kieburtz and Ishimaru.[1] Particular attention is paid to the convergence properties of the solution for the self-complementary screen.

The magnitude and phase of the reflection coefficient, Γ, for the self-complementary is shown in Figure 3, for $0.01 \leq s/\lambda \leq 0.21$, (greater than four octaves). For small aperture size, $s/\lambda \leq 0.1$, the screen is highly transmissive. As the aperture size, or frequency, is increased, the screen becomes more reflective. One observes from this figure that $|\Gamma|$ is directly

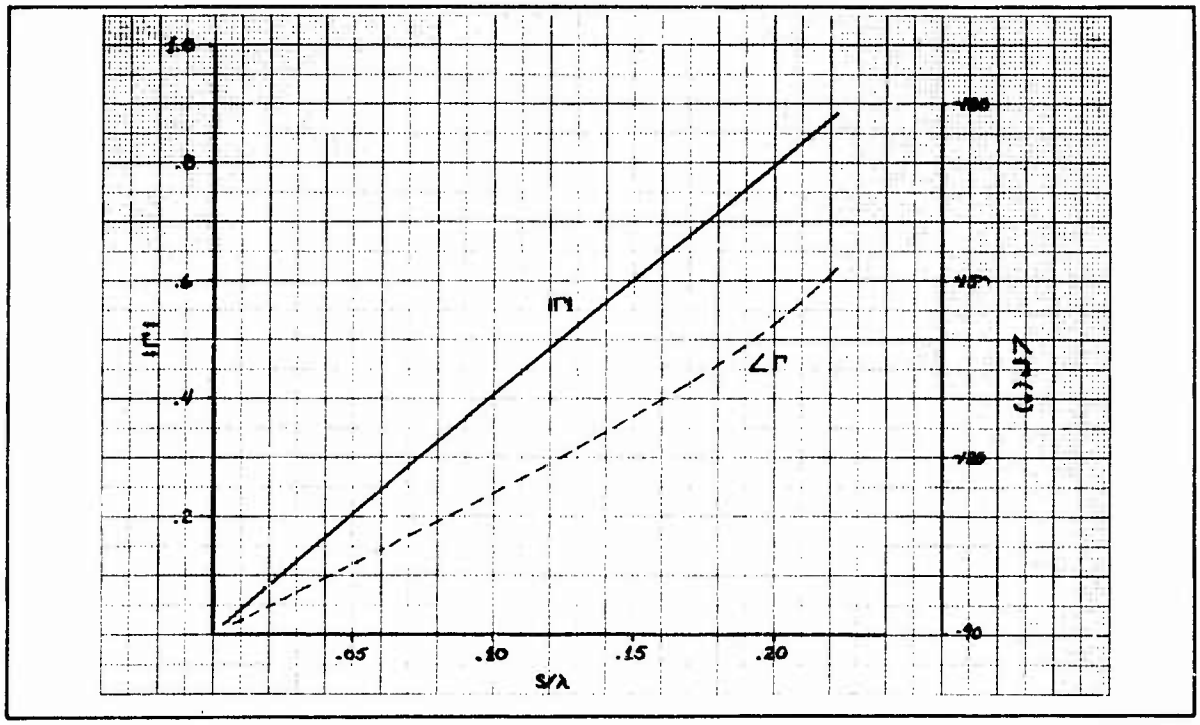

Figure 3 - Calculated Magnitude and Phase of Reflection Coefficient versus s/λ for Self-Complementary Screens (Normal Incidence)

proportional to frequency, doubling exactly for each octave for $s/\lambda \lesssim 0.1$; for $s/\lambda > 0.1$, a departure from the linearity in frequency is noted and the curve begins to bend over. In addition, the reflection coefficient phase varies approximately linearly with frequency away from -90 deg for small s/λ. This behavior is typical of a capacitive shunt susceptance whose element value is small and remains nearly constant with frequency. Although the frequency range depicted in Figure 3 is limited on the low side, the extension to lower frequencies has been studied and the results showed a continued linear frequency dependence.

As the incidence angle departs from the normal, the screen no longer presents a self-complementary structure to the incident plane wave. In both E- and H-planes, there is an effective foreshortening of the unit cell. In the H-plane it is then expected that as the incidence angle approaches 90 deg, the reflection coefficient will increase. Figure 4 shows the variation of $|\Gamma|$

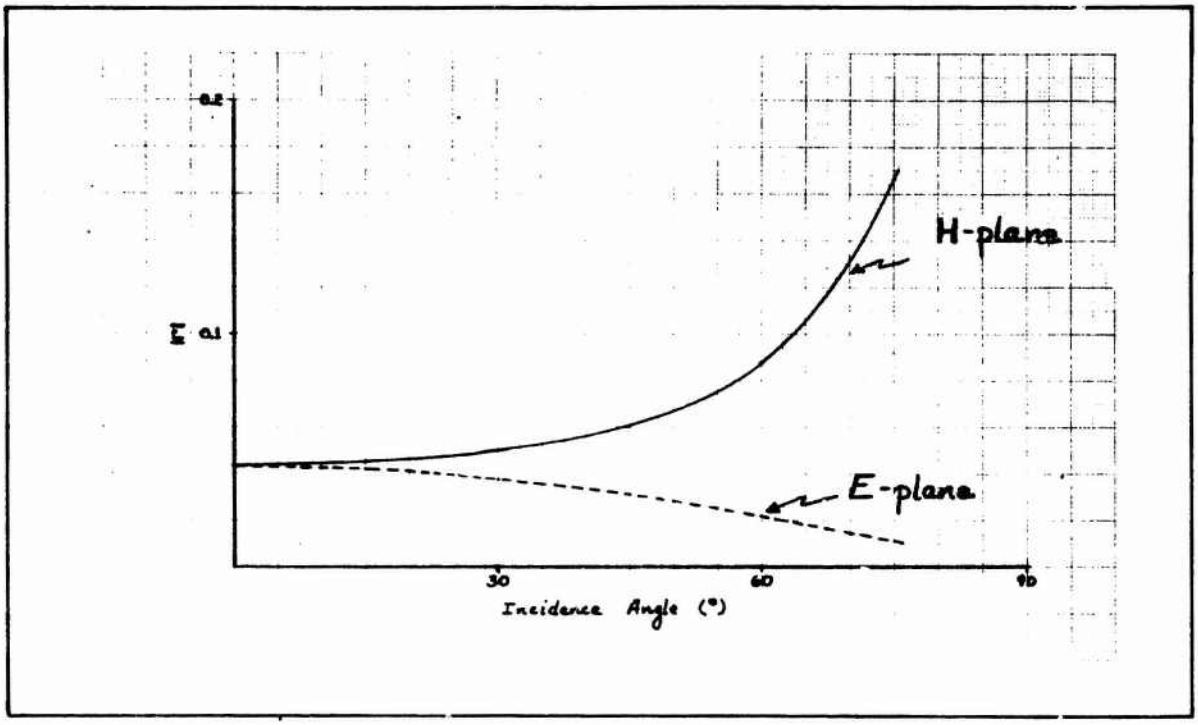

Figure 4 - Magnitude of Reflection Coefficient for E- and H-Plane Incidence on Self-Complementary Screens ($s/\lambda = 0.0106$)

with increasing incidence angle for both E- and H-plane incidence and y polarization. $|\Gamma|$ behaves in an appropriate manner in the H-plane, increasing with incidence angle. In the E-plane, $|\Gamma|$ decreases monotonically with incidence angle.

Of particular interest in the computation of $|\Gamma|$ is the convergence characteristic of equations (18). As discussed in Subsection 2.2, primary contributions to the summand in equations (18) are obtained at broadside when there are sufficient number of aperture and space functions so that for the Nth aperture mode and the Pth space mode, $P \cong N\, s_x/2A$ where only $TE_{n,o}$ aperture modes are considered. For the self-complementary screen, $s_x = 2A$; thus the periodicity of the Pth space harmonic over the cell is exactly twice the periodicity of the Nth aperture mode in the aperture. Consequently, for $P = Q = 21$, $N = 21$. The convergence of $|\Gamma|$ at broadside versus number of even symmetry aperture modes (odd symmetry modes are not excited at broadside) is shown in Figure 5 with parameter s/λ, for

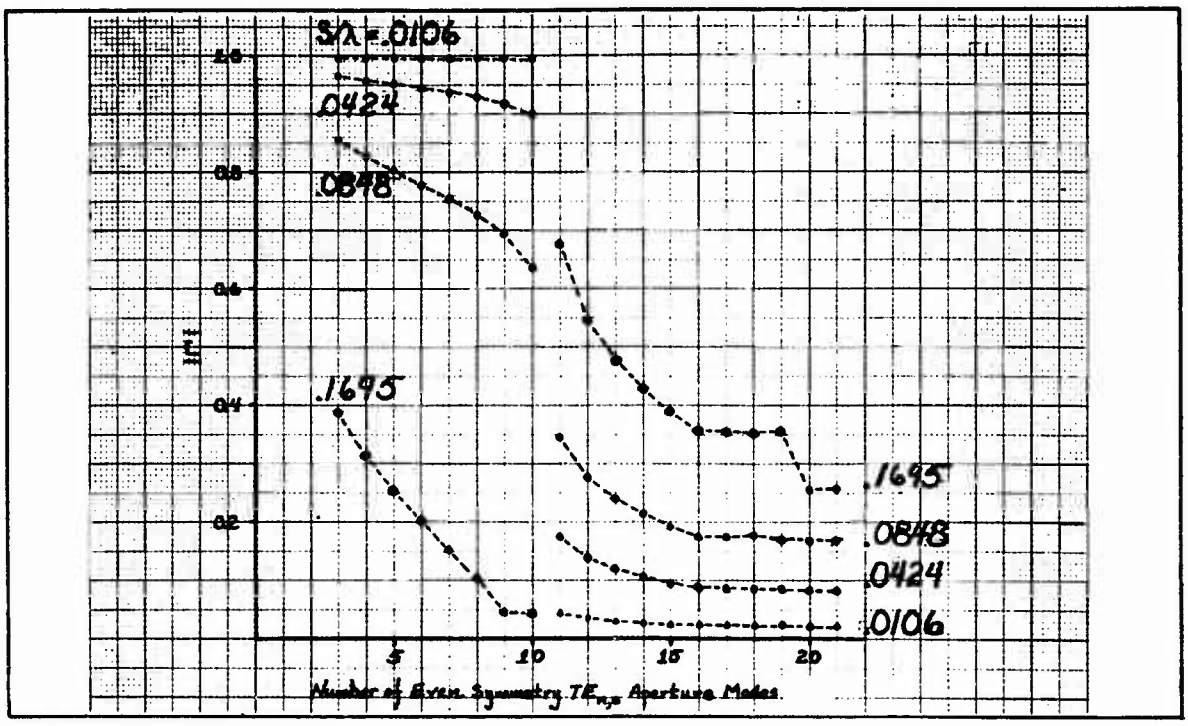

Figure 5 - Relative Convergence of $|\Gamma|$. $TE_{n,o}$ Modes.
$P = Q = 21$, $n = 2K - 1$

$P = Q = 21$. A single, well-defined discontinuity occurs on the addition of the eleventh aperture mode ($TE_{21,0}$ mode), and subsequent inclusion of modes out to the sixteenth leaves the frequency dependence of $|\Gamma|$ unchanged. The fact that the frequency dependence of $|\Gamma|$ remains unchanged upon adding more aperture modes beyond the $TE_{21,0}$ mode might suggest that an absolute convergence is being observed. However, examination of the modal voltage coefficients and the test for conservation of energy shows that:

1) The modal voltages become unphysically large as aperture modes are added beyond the $TE_{21,0}$ mode;
2) Numerically conservation of energy is exactly satisfied if and only if $P > N\ s_x/2A$ ($P \geq N$ for the self-complementary screen);
3) The aperture field distribution satisfies the edge field condition at $-A/2$ and $A/2$ if and only if $P = N$, i.e., $|V_m|$, the magnitude of the $TE_{n,o}$ mode voltage coefficient determined from equation (18), is proportional to $m^{-3/2}$, (6) where $n = 2m + 1$ and the modes are ordered in m by increasing cutoff frequency.

From these considerations, the only physically meaningful values of $|\Gamma|$ are obtained at the discontinuities (P = Q = N) in the $|\Gamma|$ curves in Figure 5. To further illustrate the significance of the proper relative truncation of the aperture and space mode sets, the magnitudes of the excited $TE_{n,o}$ mode coefficients are shown versus mode ordering number, m, for P = Q = 21 and parameter N in Figure 6 for $s/\lambda = 0.0847$. As can be seen in the figure by comparison with the ideal fall off of $m^{-3/2}$, the edge condition is satisfied only for N = 21; when n excedes 21, the coefficients of the higher order aperture modes are exponentially increasing. Examination of equation (19) shows that this exponential increase follows directly from the absence of the space harmonics for matching the most rapid variation of the aperture modes. The departure of $|V_{in}|$ from the $m^{-3/2}$ fall-off for larger m in the N = 21 curve is a measure of the error in the solution. In particular, the relative truncation of the mode sets excludes the contribution of higher order space modes to the matching of the highest order aperture modes. In this manner, the voltage coefficient of the Nth aperture mode will always be in error. However, as N is increased while maintaining relation (21), the overall fall-off of $|V_m|$ will more nearly approximate $m^{-3/2}$.

Figure 7 shows a section of an infinite periodic screen of square apertures in a square lattice. This screen has been analyzed by Kieburtz and Ishimaru[1] using a variational technique. The trial aperture distribution used was

$$\underline{e}(\underline{s}) = e_x(\underline{s})\,\hat{x} + e_y(\underline{s})\,\hat{y}$$

$$e_x(\underline{s}) = 0$$

$$e_y(\underline{s}) = [1 - (2x/s)^2]^{1/2}\,[1 - (2y/s)^2]^{1/2}$$

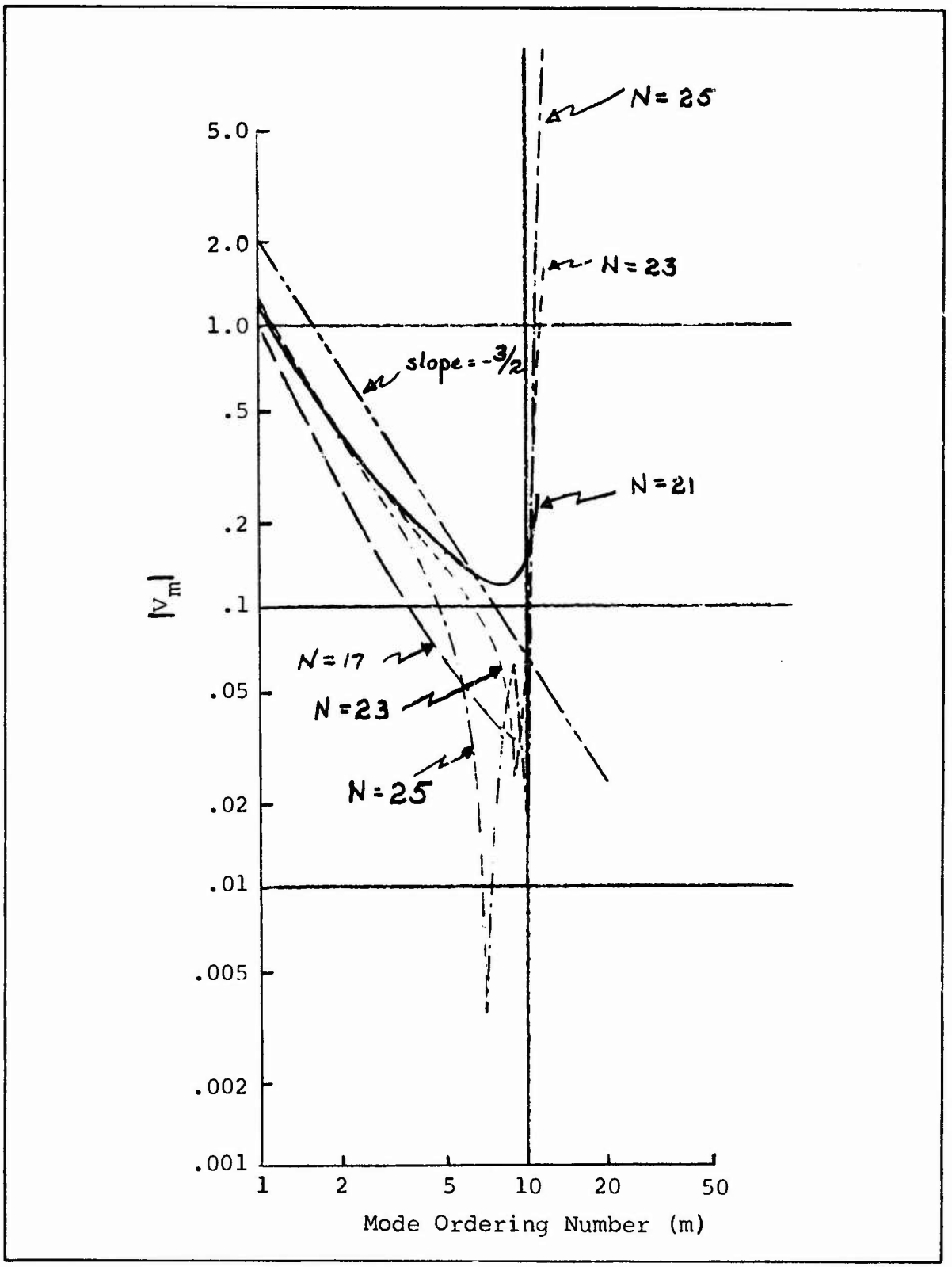

Figure 6 - Magnitude of V_m versus Mode Ordering Number (m)
P = Q = 21

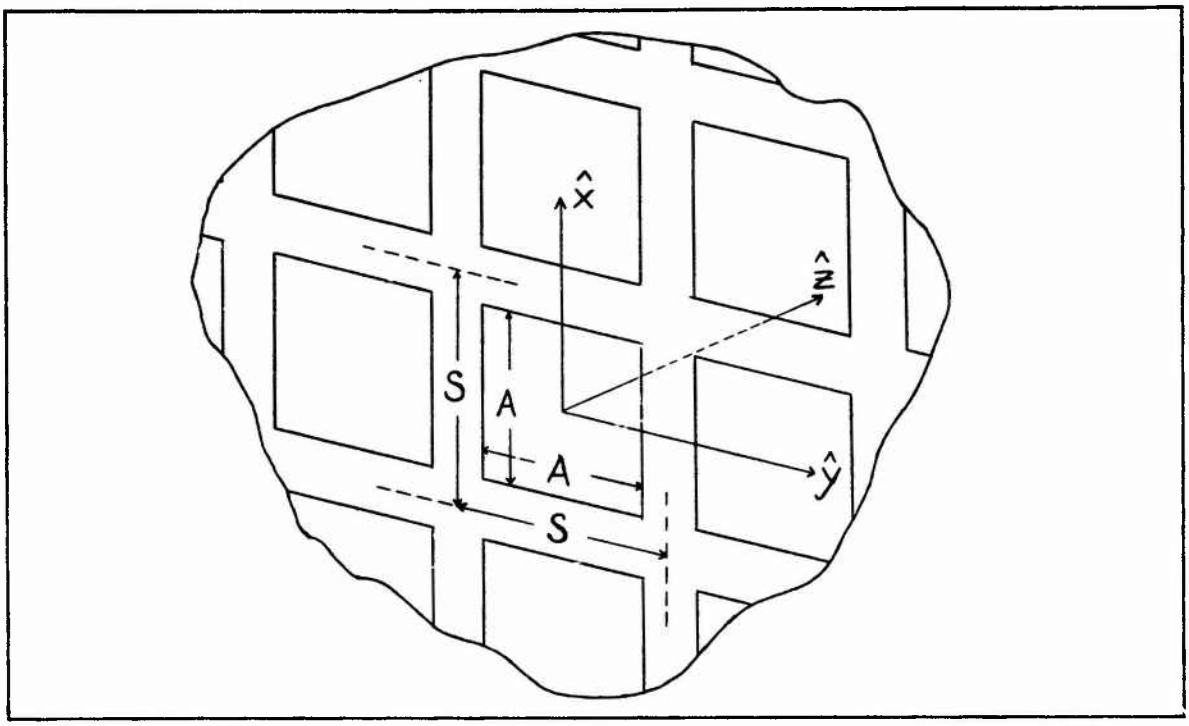

Figure 7 - Square Grid of Square Apertures

which satisfies the boundary conditions on E_y at the edges of the aperture. Figure 8 shows the voltage reflection coefficient for the square array of square apertures for broadside incidence as computed by Kieburtz and Ishimaru[1] and by the present method employing only TE modes with even symmetry. The overall agreement is excellent. The departure is due to failure to exactly satisfy the edge condition in the E-plane in the present analysis.

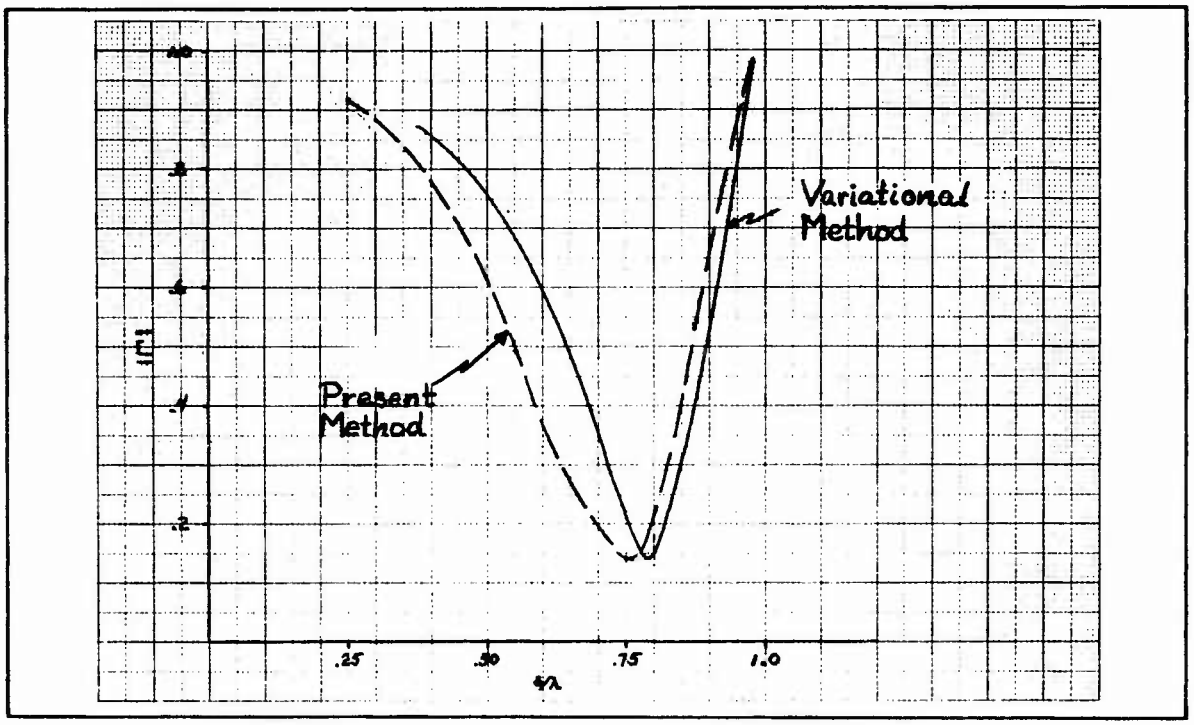

Figure 8 - Reflection Coefficient versus s/λ for Square Grid of Square Apertures ($A/s = 0.7$)

2.4 Equivalent Circuit Representation for the Self-Complementary Screen

In the preceding sections, it was demonstrated that for small s/λ ($s/\lambda \lesssim 0.21$), the self-complementary screen has characteristics similar to a shunt susceptance of small, nearly constant, capacitive element value for a normally incident plane wave. The shunt element represention follows directly from the dominant mode electric field continuity across the interface (equation (7)). The capacitive characteristic follows from the linear frequency dependence of both the magnitude and phase of Γ.

Taking z as the direction of propagation, the equivalent network representation for plane wave scattering is shown in Figure 9. From this figure, the susceptance and element value can be determined from the calculated values of reflection coefficient. The reflection coefficient, at $z = 0^-$ in Figure 9 is

$$\Gamma = \frac{-1}{1 - j2Y_o/B}$$

$$= \frac{1}{\sqrt{1 + (2Y_o/B)^2}} \exp\left[j\tan^{-1}\left(\frac{-2BY_o}{-B^2}\right)\right] \tag{22}$$

where Y_o is the free space characteristic admittance, $\frac{1}{120\pi}$ mhos. The magnitude of B is then

$$B = \frac{2Y_o\,|\Gamma|}{\sqrt{1 - |\Gamma|^2}} \tag{23}$$

From Figure 3, $|\Gamma| = 0.0437$ for $s/\lambda = 0.0106$ (f = 1 GHz) and $B = 0.000232$. Since a purely capacitive element is assumed, $B = \omega C$ and $C = 0.0369$ pF. For $s/\lambda = 0.0847$, $|\Gamma| = 0.346$, thus $B = 0.001936$ and $C = 0.0389$ pF. Over three octaves, the element value varies by only 5.4 percent. Selecting the element value obtained for $s/\lambda = 0.0106$ as the nominal capacitance of the screen (C = 0.0369 pf), the deviation from constant capacitance, as

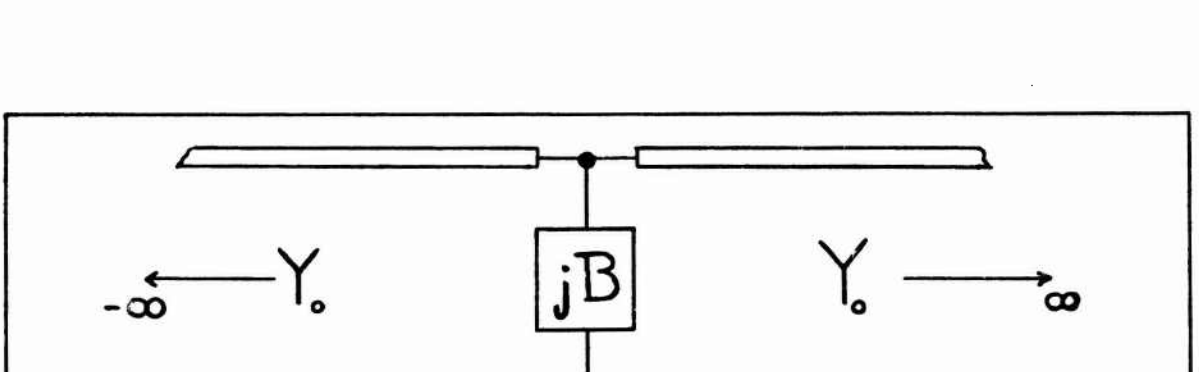

Figure 9 - Dominant Mode Equivalent Circuit for Periodic Screen of Apertures

determined from $|\Gamma|$ is shown in Figure 10. From Figure 10, it is evident that the approximation of a constant capacitive shunt element is reasonably valid out to $S/\lambda \cong 0.19$.

From equation (22) the phase of $|\Gamma|$ lies within the range $-\pi \leq \phi \leq -\pi/2$ and is given by

$$\phi = \tan^{-1} \frac{2Y_o}{\omega C} - \pi \tag{24}$$

For values of capacitance on the order of 0.0369 pF, and frequencies in the range of interest (1 - 10 GHz),

$$\phi \cong -\frac{\pi}{2} - \frac{\omega C}{2Y_o} \quad . \tag{25}$$

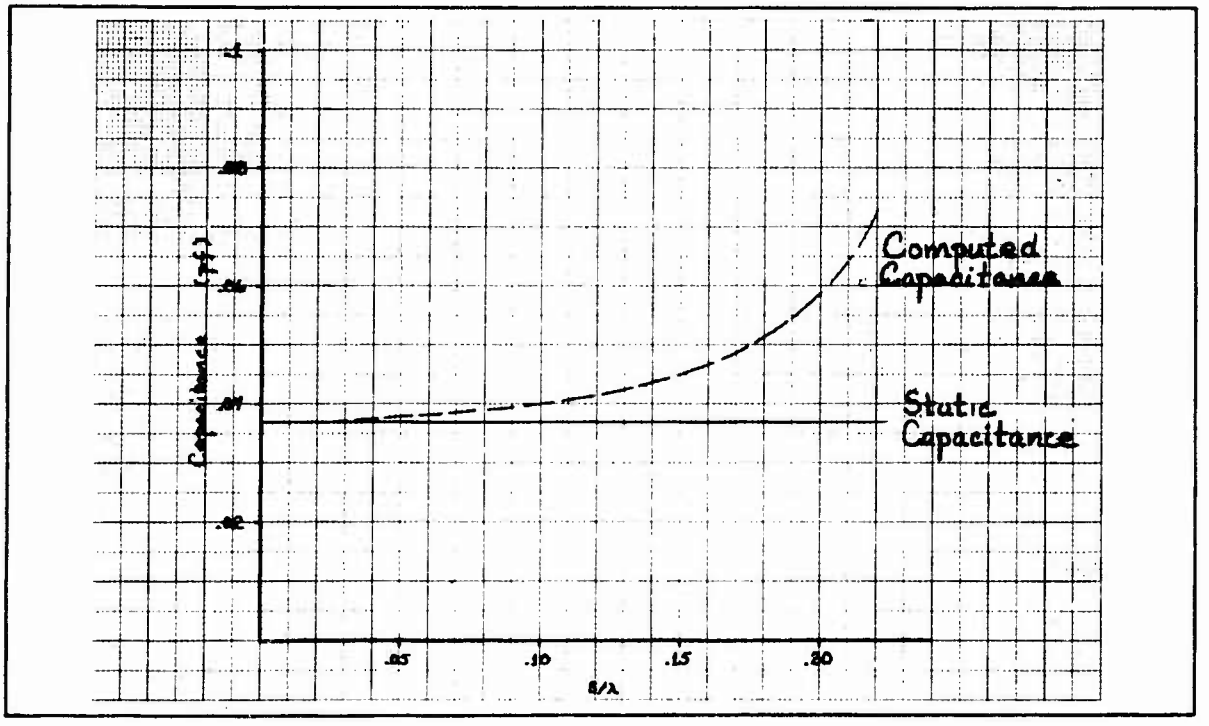

Figure 10 - Self-Complementary Screen Capacitance versus s/λ ($s = 0.125$ in.)

The linear frequency dependence of ϕ holds only for low frequencies since the arctangent approximation (25) is only valid for large arguments. Selecting C = 0.0369 pF as the nominal capacitance of the screen, the percentage deviation of the phase of Γ(shown in Figure 3) from the phase obtained via equation (24) for the nominal capacitance is shown in Figure 11. As with the magnitude of reflection coefficient, phase errors in assuming a constant capacitive element occur for larger s/λ. In the range of interest the maximum error is 11.7 percent, occuring for $s/\lambda = 0.21$.

2.5 Scattering from Dielectric-Slab Covered Self-Complementary Screens

2.5.1 General Remarks

In Subsection 2.1, the general theory of scattering from thin periodic screens of rectangular apertures was developed. In Subsections 2.3, and 2.4, it was demonstrated that for normally incident plane waves the self-complementary screen of small apertures ($s/\lambda \lesssim 0.2$) presents a shunt susceptance (by virtue of dominant mode electric field continuity at the

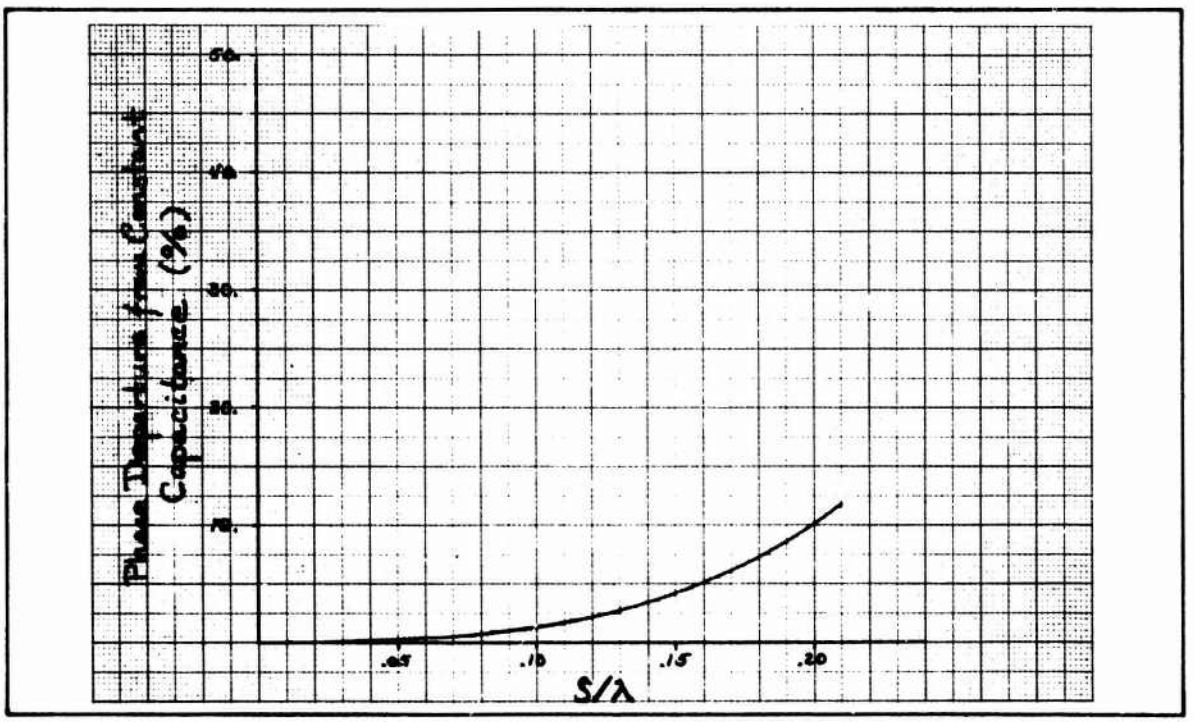

Figure 11 - Percent Phase Departure from Assumed Constant Capacitance Screen versus s/λ (s = 0.125 in.)

aperture) for which the element value is capacitive, small, and nearly constant over a wide frequency regime. In addition, it was demonstrated in Subsection 2.4, that having determined an appropriate element value for the screen, the general scattering problem may be reduced to an equivalent circuit representation. The equivalent circuit representation with constant shunt capacitance was shown to give excellent agreement with the rigorously computed results over the entire frequency regime of interest.

In practice, self-complementary screens are used in combination with a supporting dielectric slab. For thin slabs of moderate or small relative permittivity, the screen-slab combination will look essentially like the screen alone. However, for thick slabs (of the order of a half wavelength in the dielectric) the screen can strongly effect the reflection and transmission characteristics of the slab. Of particular significance for thicker dielectrics (such as might be used for microwave radome applications) is whether or not the screen in combination with the slab can improve the transmission bandwidth. Results of the current study show that the self-complementary screen, when used in combination with a thick dielectric slab, will not give an increase in bandwidth over the slab alone.

The analytical techniques developed in Subsection 2.1 may be extended to include multiple dielectric regions through relatively simple transformations of the resultant solution (equation (18)) to include the appropriate admittance variations of the media. For the dielectric-slab covered screen geometry shown in Figure 12, it is seen that the structure separates into three regions, each characterized by a different transverse to z cross section or medium. For $z < 0$ and $z > h$, the media are free space; $z = 0$ is the plane of the screen of rectangular apertures; and for $0 < z < h$ the dielectric slab is present. The scattering properties of the slab-covered screen are determined from a formulation involving the scattering at the individual discontinuities: at $z = 0$ for the dielectric half-spaces separated by the screen; and at $z = h$, for the dielectric slab-free space interface. The scattering of the screen separated dielectric half-spaces is simply an extension of the formulation presented in Subsection 2.1. The dielectric half-space interface presents a simple impedance discontinuity and does not introduce mode coupling. The discontinuities may then be related by appropriate transmission lines.

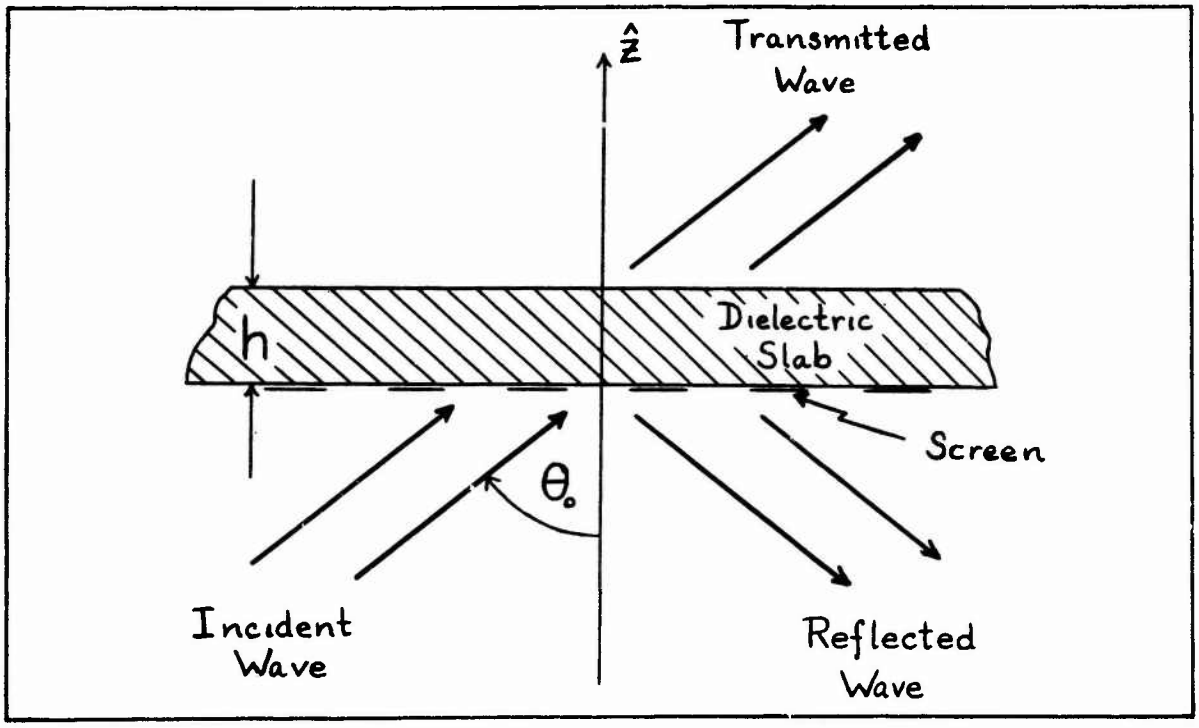

Figure 12 - Geometry of Dielectric Slab Covered Screen

However, for a small aperture ($s/\lambda \lesssim 0.2$) self-complementary screen covered by a dielectric slab, the discussion in Subsection 2.4 of the characteristics of the screen embedded in free-space suggests an equivalent circuit approach. In the three regions of Figure 12, only the dominant mode is propagating, even for moderately large values of dielectric constant in the slab region. For dominant mode propagation the slab covered screen may be characterized by an equivalent circuit developed by incorporating the shunt capacitance for the screen as determined in Subsection 2.4. In the range of validity of the constant value of capacitance, and single mode propagation, the circuit representation predicts the reflection properties of the configuration with extremely good agreement (over a three octave bandwidth).

2.5.2 Equivalent Circuit Representation for Dielectric-Slab Covered Self-Complementary Screens

For small aperture self-complementary screens ($s/\lambda \lesssim 0.21$), it has been demonstrated that an equivalent network representation may be

developed to determine the normal incidence, dominant mode scattering characteristics of the structure when embedded in free-space. In particular, it was shown that for $s/\lambda \lesssim 0.21$, the screen may be represented as a small, nearly constant, shunt capacitive element across an infinite transmission line. Similarly, the scattering at normal incidence from a dielectric slab covered screen may be represented by the capacitance at the screen discontinuity, a length of line with its appropriate admittance, and free-space admittance termination. The equivalent network representation of the dielectric slab-covered self-complementary screen is shown in Figure 13, where z is taken as the direction of propagation, h is the line length corresponding to slab thickness, and Y_o and Y_ϵ are the characteristic admittances of free-space and the dielectric slab, respectively. The capacitive element value of the shunt susceptance, B, is determined from the reflection coefficient of the free-space embedded screen, as in Subsection 2.4 and is given by

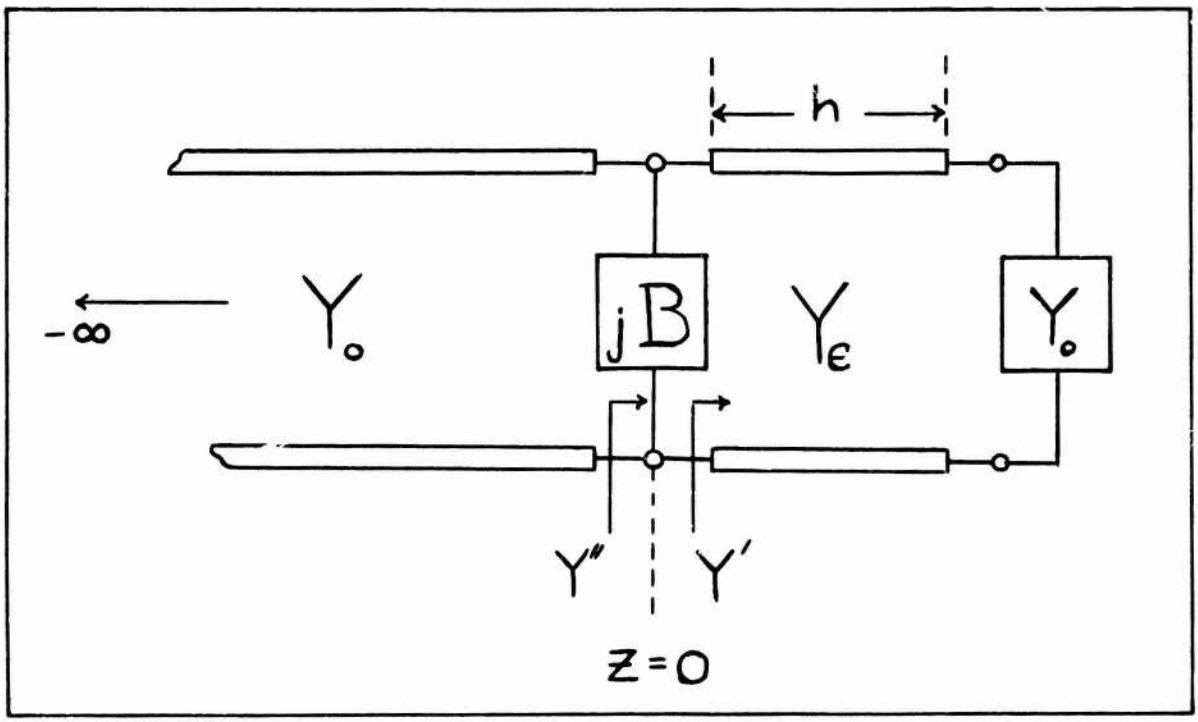

Figure 13 - Dominant Mode Equivalent Circuit for Dielectric Slab Covered Periodic Screen of Apertures

$$B = \frac{2Y_o |\Gamma|}{\sqrt{1 - |\Gamma|^2}} = \omega C \tag{26}$$

where $|\Gamma|$ is associated with a particular frequency, ω. In comparison with experiment, it was found that the best agreement was obtained when $|\Gamma|$ was chosen for very small ω, (i.e., as the dynamic solution approached the static limit corresponding to the region in which C differs immeasureably from a constant with respect to large changes in frequency).

Taking z = 0 as the location of the shunt element the admittance at $z = 0^+$ looking toward positive z is

$$Y' = Y|_{z = 0^+} = Y_\epsilon \frac{Y_o - jY_\epsilon \tan(-k_\epsilon h)}{Y_\epsilon - jY_o \tan(-k_\epsilon h)} \tag{27}$$

where k_ϵ is the wave number in the dielectric, given as $k_\epsilon = 2\pi\sqrt{\epsilon_r}/\lambda_o$ and ϵ_r is the relative permittivity of the dielectric. Then at $z = 0^-$

$$Y'' = Y' + jB \tag{28}$$

and the reflection coefficient for the dielectric slab covered screen is

$$\Gamma \cong \Gamma'' = \frac{Y_o - Y''}{Y_o + Y''} \tag{29}$$

Of particular interest in the study of the self-complimentary screens is determining their potential as broadband matching devices for radomes at microwave frequencies. In practical microwave radome design the thickness of the radome is of the order of $\lambda/2$, as measured in the dielectric. For purposes of determining if any bandwidth benefits are forthcoming with the screen, an X-band radome design was carried out.

The bandwidth of the radome is arbitrarily defined such that the VSWR does not exceed 1.5 ($|\Gamma| \leq 0.2$) and the design center frequency is taken as 11.35 GHz. Using Missilex-6 ($\epsilon_r = 6$) as the dielectric, the

admittance response for the dielectric slab and dielectric-screen combination are shown in Figure 14 for a 0.03125 in. square aperture screen of 0.00923 pF equivalent capacitance. For the dielectric alone, the thickness of the slab is 0.2123 in. ($h/\lambda = 0.5$). For the dielectric-screen combination, the slab thickness is 0.20412 in. ($h/\lambda = 0.481$) such that the added capacitance provides mid-band resonance. To remain below 1.5 VSWR, the frequency spread for the dielectric-screen combination is 10.627 GHz to 12.071 GHz or about 12.72 percent around 11.35 GHz; for the slab alone, the spread is 10.624 GHz to 12.076 GHz, or 12.79 percent around 11.35 GHz. In general, the presence of the screen tends to decrease bandwidth with respect to the simple slab. In addition, the self-complimentary screen suitable to bring about resonance in this example has an excessively small aperture size, making its implementation impractical. Larger aperture screens have proportionally larger equivalent capacitance which will tend to further reduce the bandwidth with respect to the dielectric slab alone.

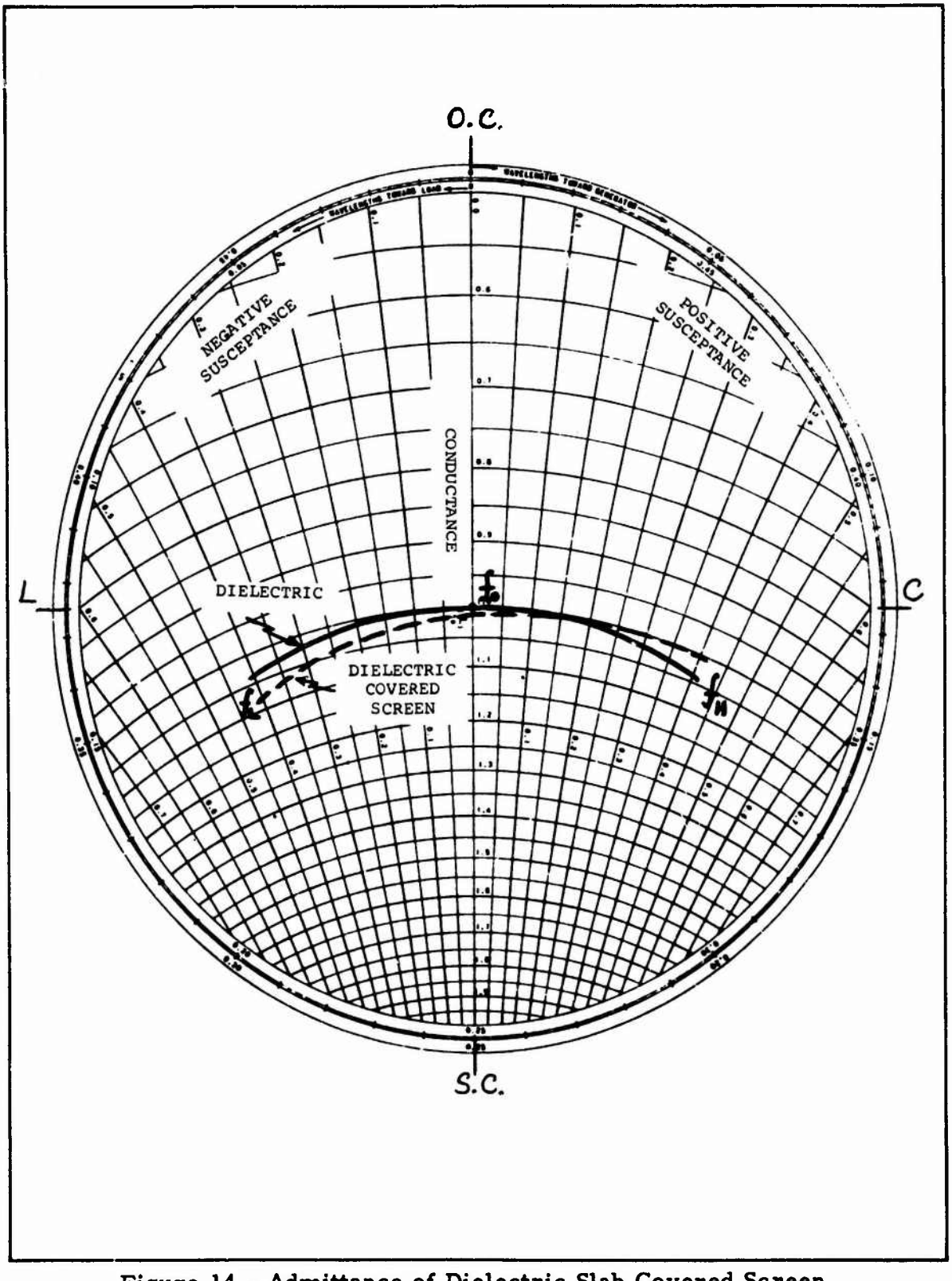

Figure 14 - Admittance of Dielectric Slab Covered Screen ($h/\lambda_o = 0.481$) Resonant at λ_o Compared to Admittance of Dielectric Slab ($h/\lambda_o = 0.5$)

3. EXPERIMENTAL INVESTIGATION

3.1 Experimental Program

An experimental program has been conducted to check the validity of the theoretical results. The agreement between theory and experiment is excellent over the range $0.02 < s/\lambda < 0.2$, or about 3 octaves. In the experiments, VSWR was measured in a matched, large aperture feed horn with the aperture covered by several different dielectric slab covered self-complementary screens.

Two large aperture horns were used to determine the bandwidth characteristics of the self-complementary screen. Over the range 8 GHz to 18 GHz, the 4 in. square aperture horn shown in Figure 15 was used. Over the remainder of the experimental band, the horn aperture was 4.295 in. x 2.134 in. The angle of plane wave incidence at the aperture (corresponding to H-plane incidence on the screen) is shown versus frequency for the two horns in Figure 16. VSWR was measured for three self-complementary screens: 0.125 in. square apertures with a 0.03125 in. thick Duroid Slab ($\epsilon_r = 2.35$); 0.0625 in. square apertures with 0.03125 in. thick Duroid slab; and 0.125 in. square apertures with 0.0625 in. thick Missilex -6* slab ($\epsilon_r = 6.$).

3.2 Plane Wave Reflection by Dielectric Slab Covered Self-Complementary Screens - Measured

In this subsection, the measured VSWR data is presented. The measured VSWR data has been smoothed and the corresponding reflection coefficients are compared with calculations based on the theory developed in Subsection 2.5 for the dielectric slab covered self-complementary screen.

The measured VSWR is shown in Figures 17 through 22. No data was obtained for the Missilex -6 covered screen over the range 8 to 12.4 GHz. The ripples in the curves are asociated with the horn transitions, as seen

*A high temperature dielectric product of Custom Materials Co.

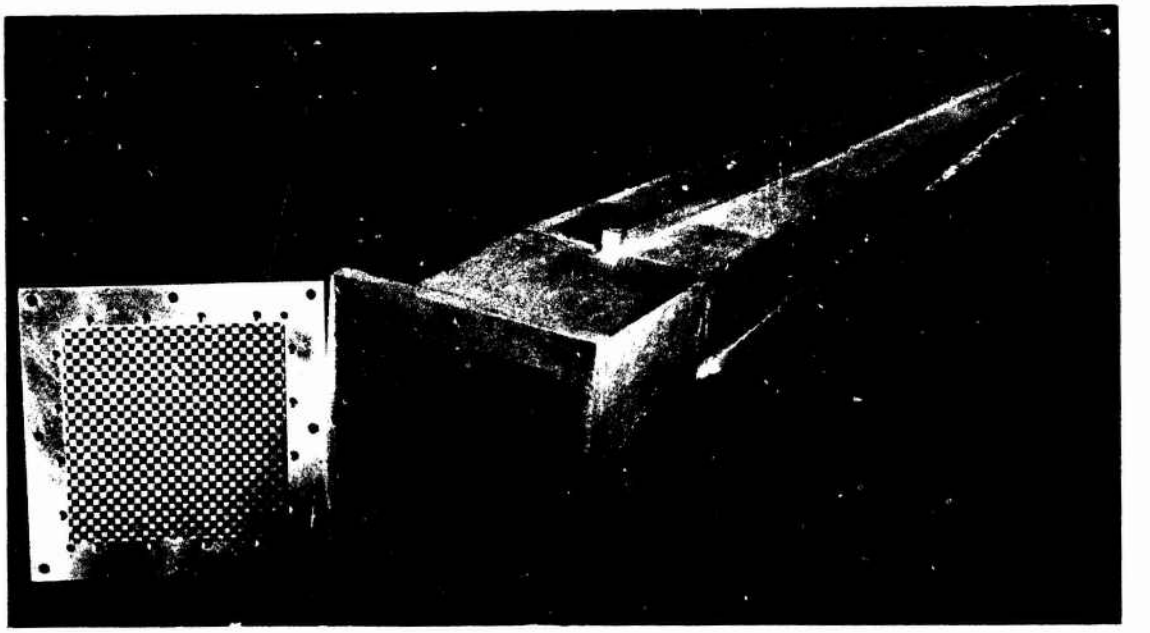

Figure 15 - Dielectric Slab Covered Self-Complementary Screen and 4 in. Square Horn

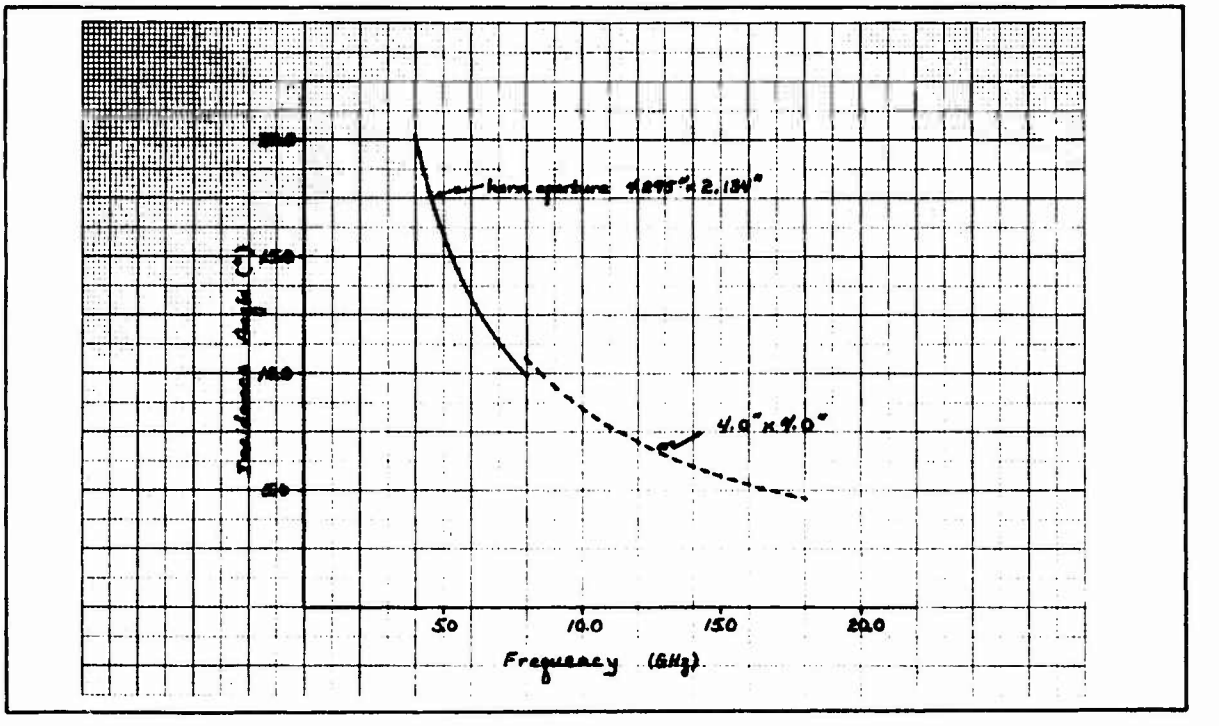

Figure 16 - Incidence Angle versus Frequency for Experimental Horns

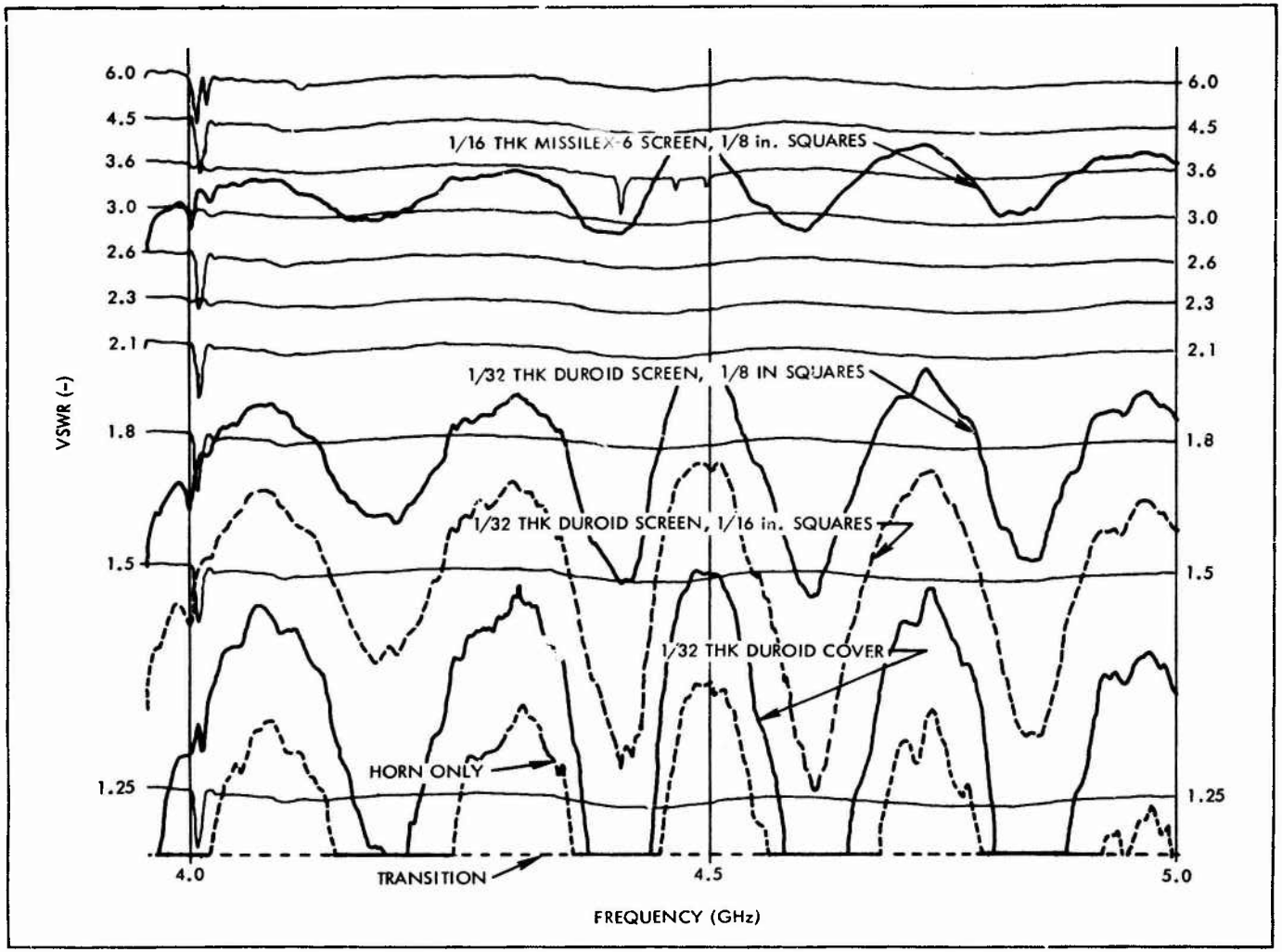

Figure 17 - Measured VSWR versus Frequency for 0.03125 in. Thick Duroid Slab Covered Self-Complementary Screens of 0.0625 in. and 0.125 in. Apertures and 0.0625 in. Thick Missilex-6 Slab Covered Self-Complementary Screen of 0.125 in. Apertures

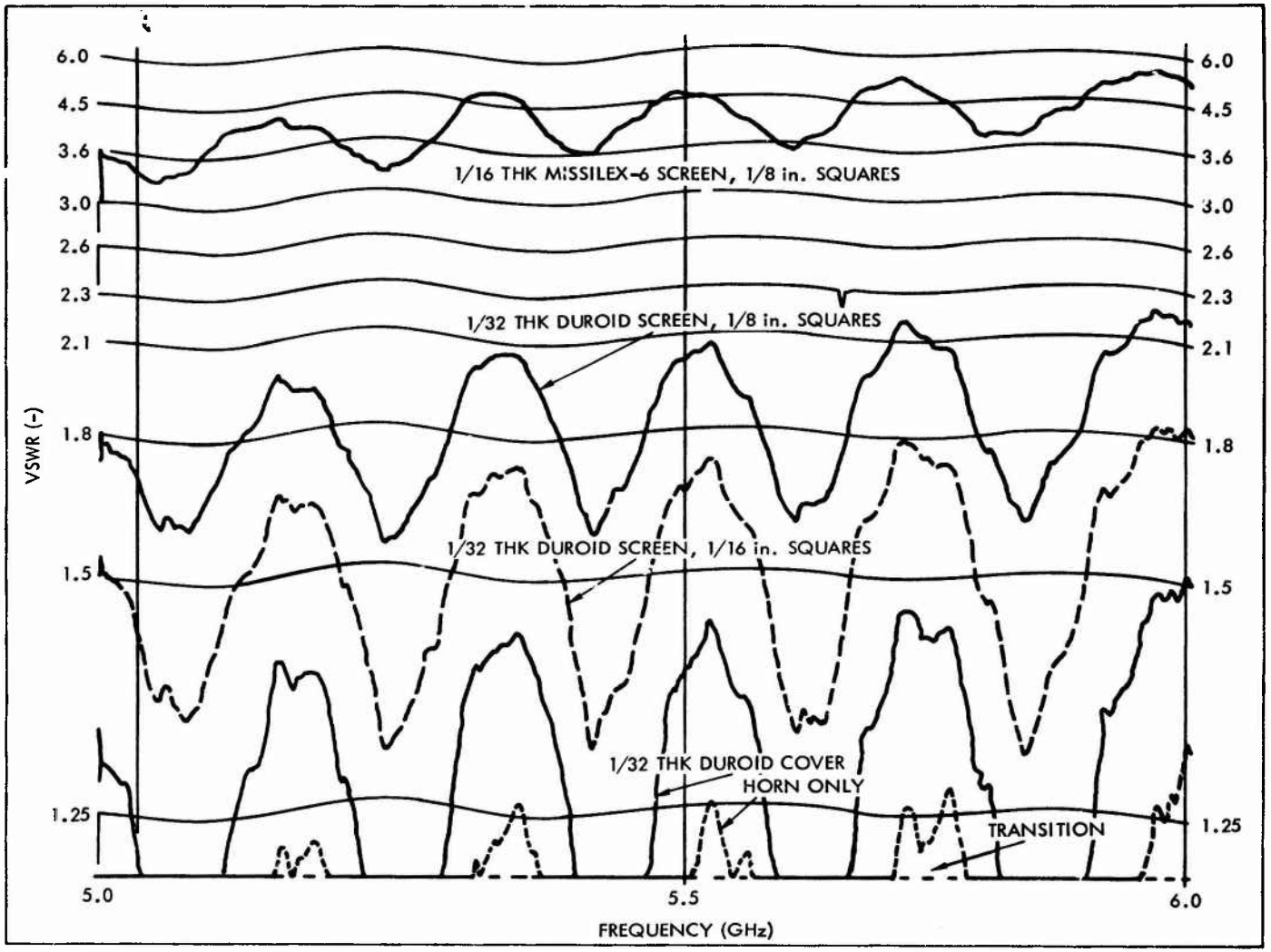

Figure 18 - Measured VSWR versus Frequency for 0.03125 in. Thick Duroid Slab Covered Self-Complementary Screens of 0.0625 in. and 0.125 in. Apertures and 0.0625 in. Thick Missilex-6 Slab Covered Self-Complementary Screen of 0.125 in. Apertures

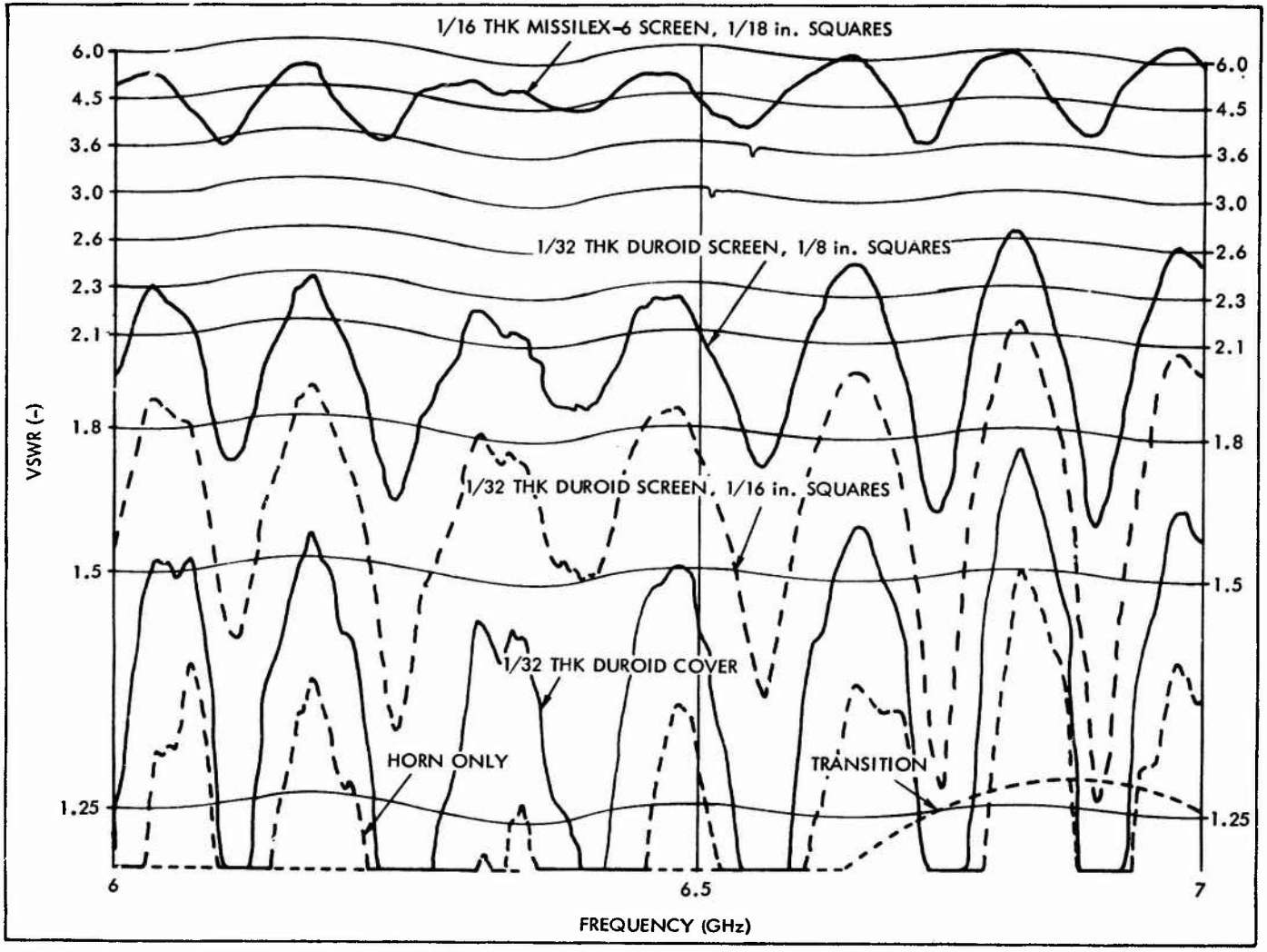

Figure 19 - Measured VSWR versus Frequency for 0.03125 in. Thick Duroid Slab Covered Self-Complementary Screens of 0.0625 in. and 0.125 in. Apertures and 0.0625 in. Thick Missilex-6 Slab Covered Self-Complementary Screen of 0.125 in. Apertures

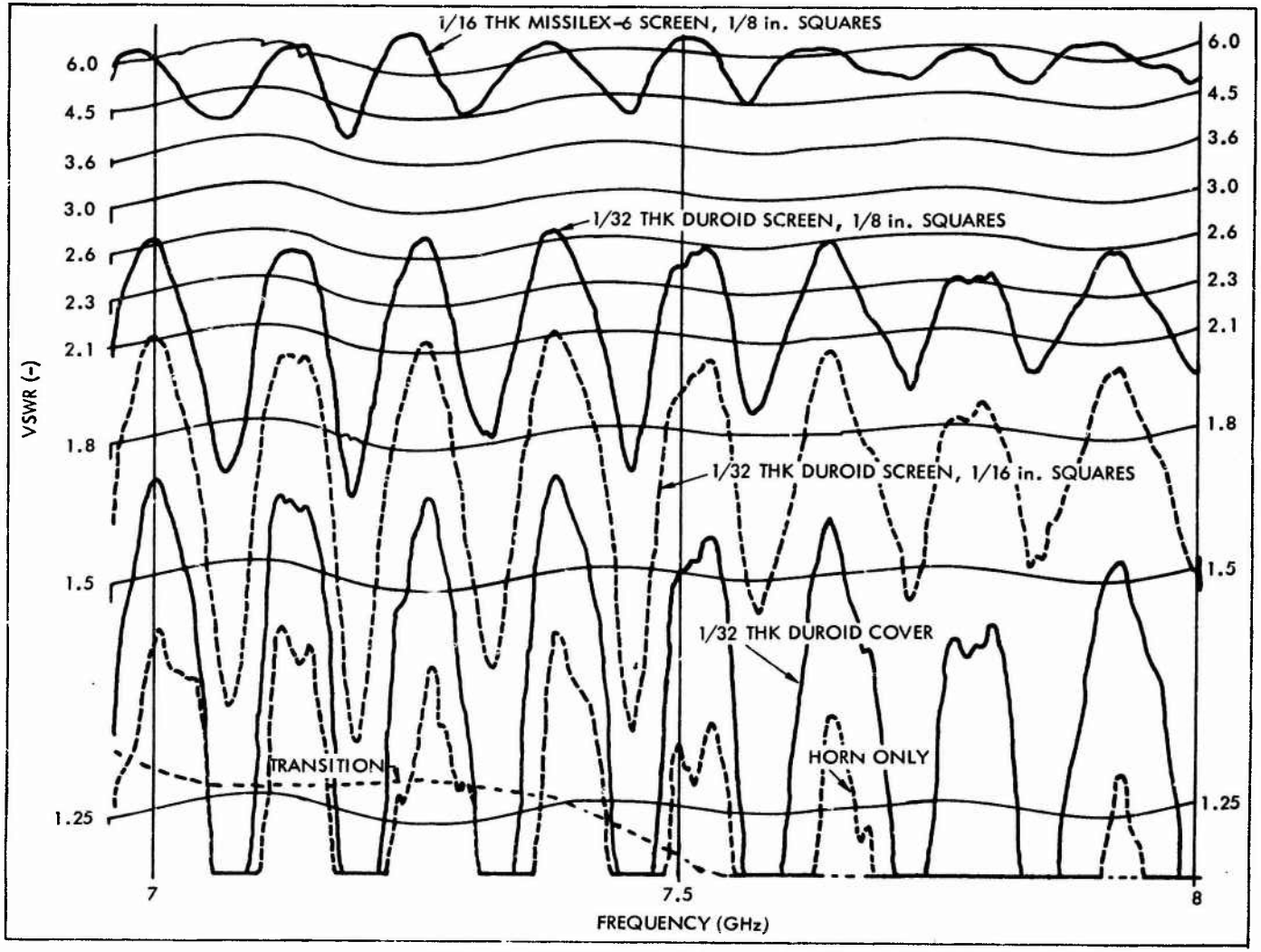

Figure 20 - Measured VSWR versus Frequency for 0.03125 in. Thick Duroid Slab Covered Self-Complementary Screens of 0.0625 in. and 0.125 in. Apertures and 0.0625 in. Thick Missilex-6 Slab Covered Self-Complementary Screen of 0.125 in. Apertures

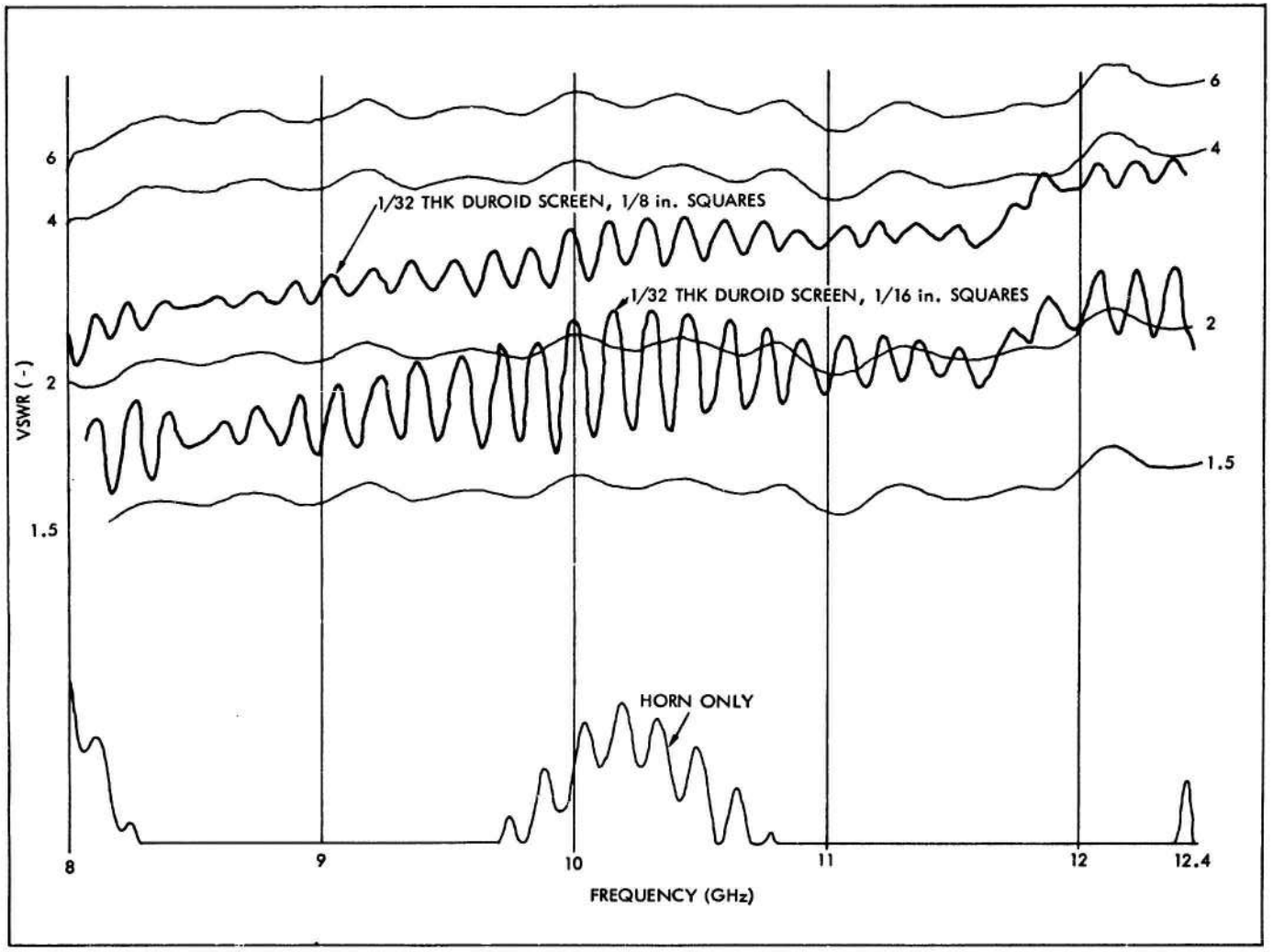

Figure 21 - Measured VSWR versus Frequency for 0.03125 in. Thick Duroid Slab Covered Self-Complementary Screens of 0.0625 in. and 0.125 in. Apertures and 0.0625 in. Thick Missilex-6 Slab Covered Self-Complementary Screen of 0.125 in. Apertures

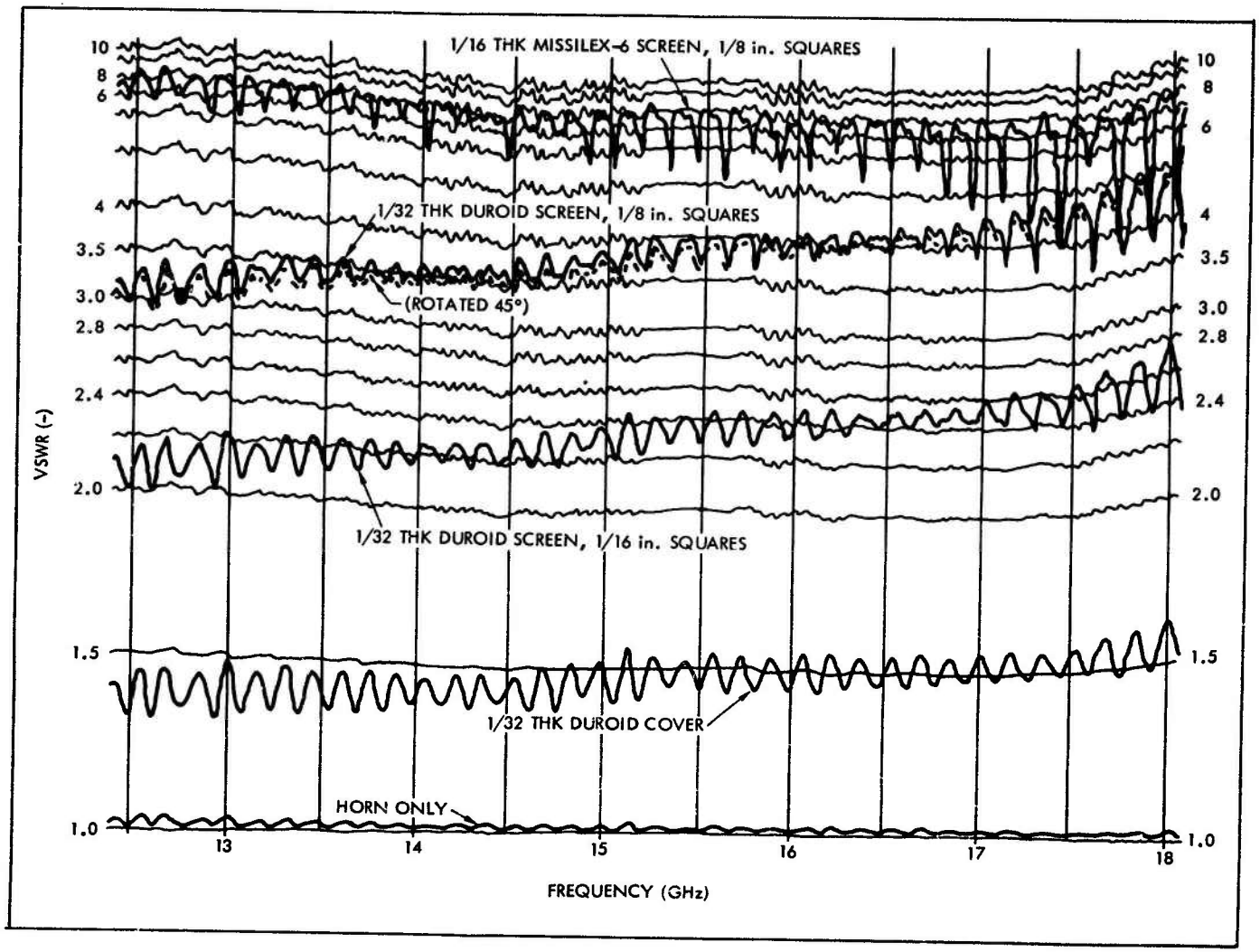

Figure 22 - Measured VSWR versus Frequency for 0.03125 in. Thick Duroid Slab Covered Self-Complementary Screens of 0.0625 in. and 0.125 in. Apertures and 0.0625 in. Thick Missilex-6 Slab Covered Self-Complementary Screen of 0.125 in. Apertures

from the curves for the horn alone and the expanded curve for the horn alone in Figure 23. The smoothed measured VSWR versus frequency for the three screens are shown in Figure 24. Over the frequency range, the VSWR is increasing with frequency for screens with low dielectric covering, while a VSWR maximum is evident at about 14.5 GHz (or $h/\lambda \approx 0.18$) for the Missilex -6 covered screen.

The first reflection coefficient maximum for normal plane wave incidence on a dielectric slab occurs for $h\sqrt{\epsilon_r}/\lambda_o = h/\lambda = 0.25$. For the Duroid slab used, the maximum h/λ in the experimental frequency range is $h/\lambda = 0.073$, and the operating range is well removed from the reflection maximum. For the Missilex -6 slab, the maximum h/λ is 0.233 (i.e., in the region of the reflection peak). The capacitive screen susceptance tends to move the reflection peak into the experimental frequency range.

Figure 25 shows a comparison between measured $|\Gamma|$ for the Missilex -6 covered screen and $|\Gamma|$ calculated from the equivalent transmission line circuit with the screen taking the constant capacitive values of 0.0369 pF as determined from Figure 3 for $s/\lambda = 0.0106$. The overall agreement between measured and computed $|\Gamma|$ is excellent. The location of the reflection coefficient peak is in the region where the experimental angle of incidence is only 6 deg from the screen normal and the error in assuming normal incidence via the transmission line approximation is very small.

Over the frequency range in the experiment, the incidence angle (corresponding to H-plane incidence) varied from approximately 20 deg (at 4 GHz) to 4.7 deg (at 18 GHz) with respect to the screen normal. In the dielectric, this results in a range of approximately 12.9 deg to 3.1 deg for the Duroid slabs and approximately 8 deg to 1.9 deg for the Missilex -6 slab. From Figure 4, it is seen that in the H-plane, $|\Gamma|$ remains approximately constant out to 35 deg with respect to the normal. The transmission line approximation, although valid only for normal incidence, should give good agreement with experiment.

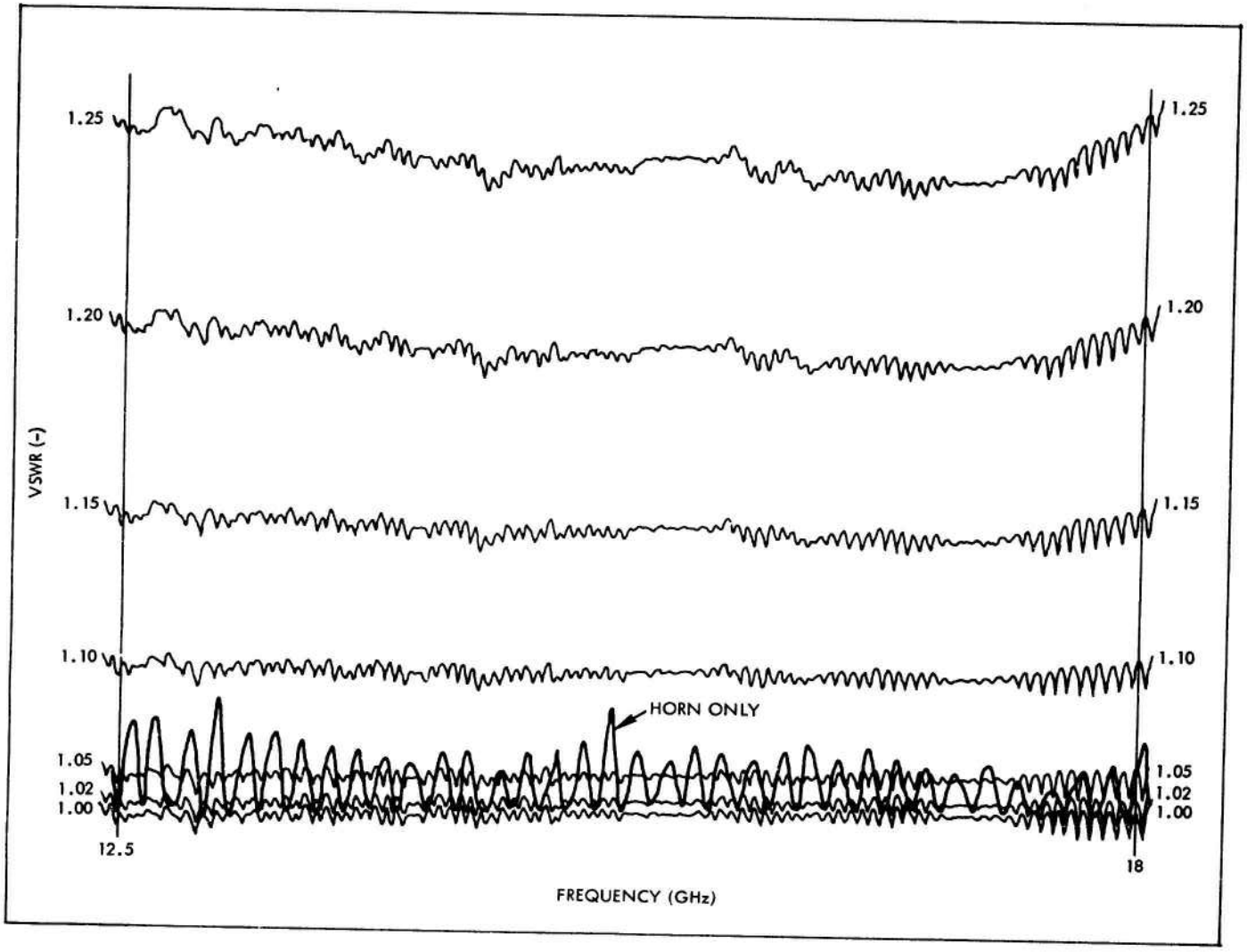

Figure 23 - VSWR versus Frequency of Uncovered 4 in. Square Horn

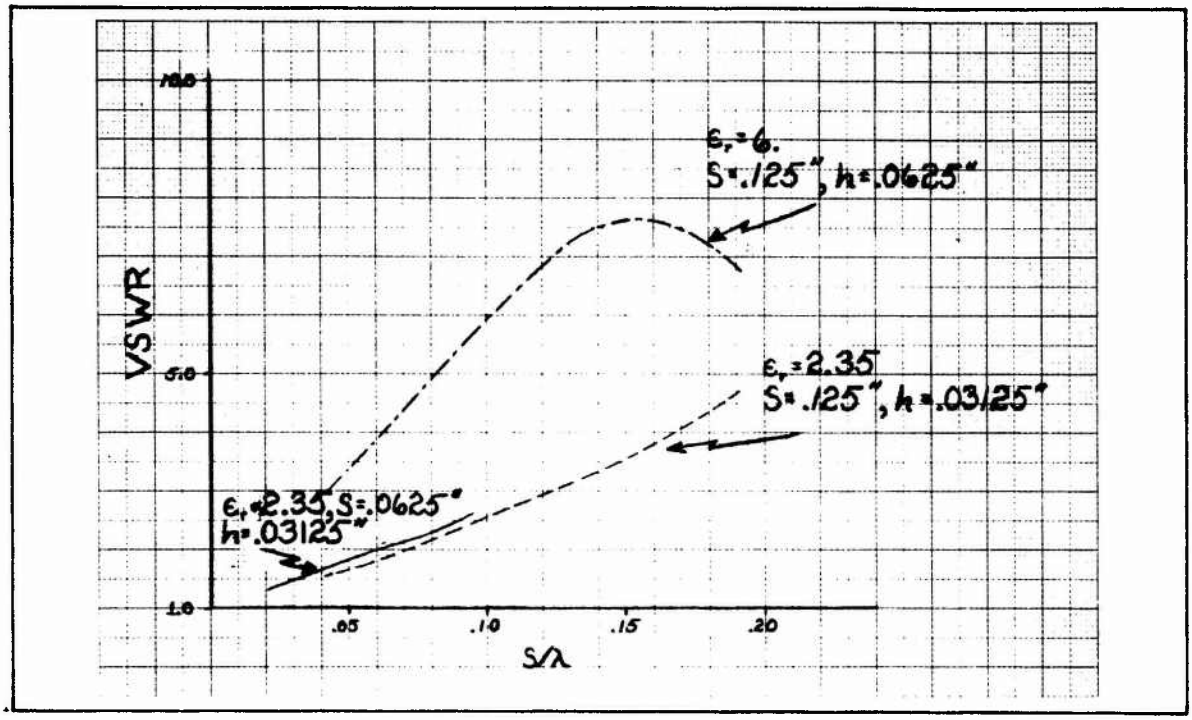

Figure 24 - Smoothed VSWR Data from Screen Covered Horn Measurements

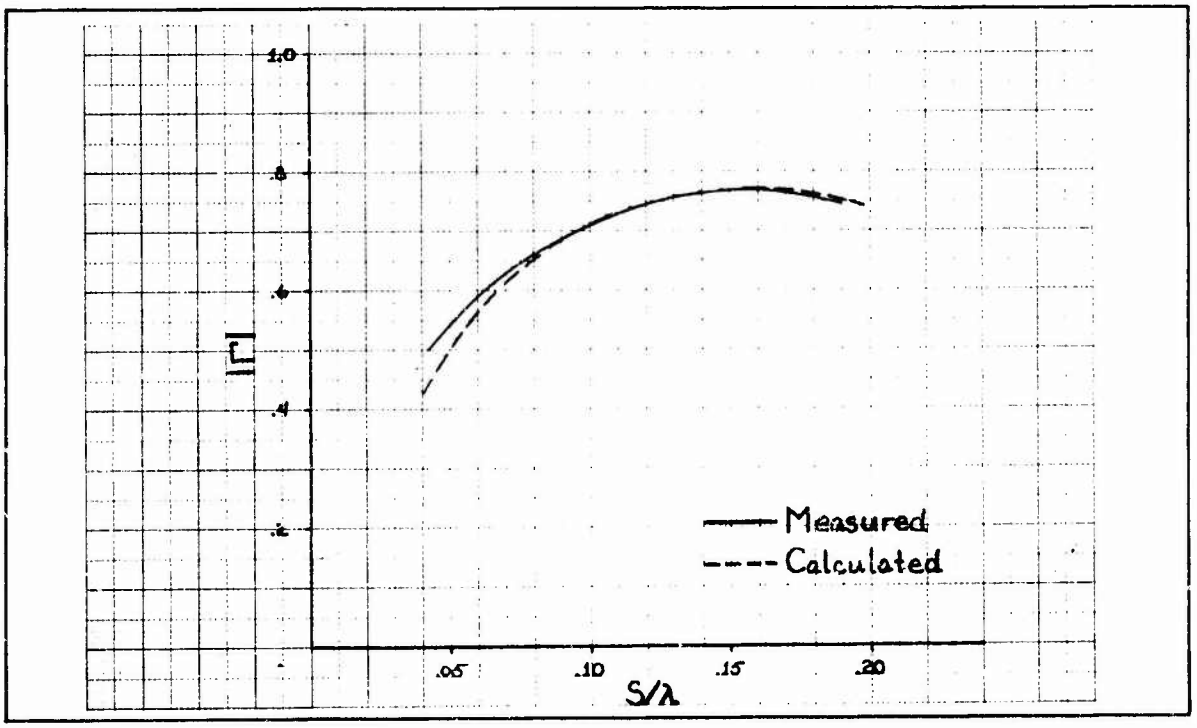

Figure 25 - Measured and Calculated Reflection Coefficient Magnitude for Missilex-6 Covered Self-Complementary Screen
(s = 0.125 in., h = 0.0625 in.)

Figure 26 shows measured and calculated $|\Gamma|$ for the two Duroid covered screens over the frequency band. The screen equivalent capacitance is taken as 0.0369 pF for the 0.125 in. square aperture screen and 0.0185 pF for the 0.0625 in. square aperture screen. The agreement between theory and measurement is excellent.

Over a portion of the experimental frequency band, the 0.125 in. square aperture screen with the Duroid slab was rotated 45 deg with respect to the incident polarization to examine affects of skew polarization. As can be seen in the raw VSWR data of Figure 22, the rotation had negligible effect, as anticipated.

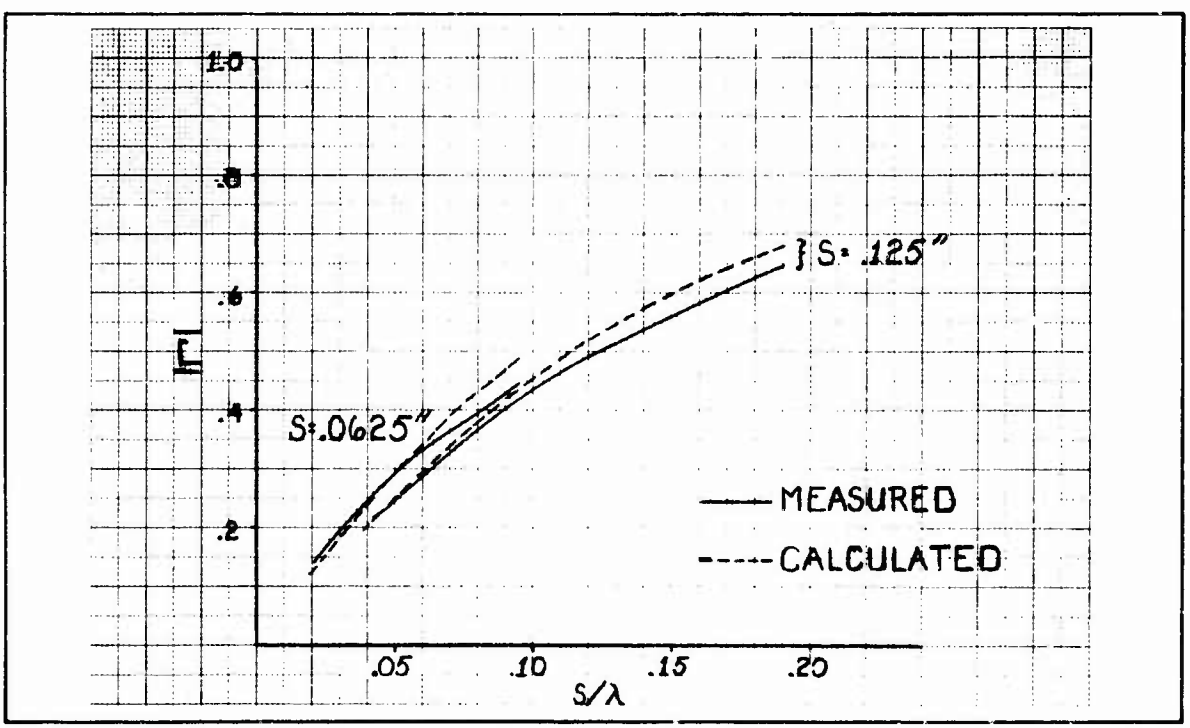

Figure 26 - Measured and Calculated Reflection Coefficient Magnitude for Duroid Covered Self-Complementary Screens
(h = 0.03125 in., s = 0.0625 in., 0.125 in.)

4. CONCLUSIONS

Self-complementry screens appear to offer no matching benefits for broadbanding radomes. However, the static capacitance associated with the structure remains essentially constant for screen apertures that are less than approximately $\lambda/4$. In this regime, the shunt susceptance associated with the screen may be useful as an element of a filter section for waveguide devices. The low pass characteristic also suggests the use of the screen for waveguides or radomes as harmonic filters, up to the region of screen aperture resonance.

In the analysis for the screen, an approximation was used to develop a convergent form of the kernel. The consequence of this approximation is to ignore higher order intermode coupling. The formalism that is evolved is rather simple, and the excellent agreement with experiments suggests that this approximation may be useful for similar iris or diaphragm solutions.

REFERENCES

1) Kieburtz, R.B., and Ishimaru, A., "Scattering by a Periodically Apertured Conducting Screen", IRE Transactions on Antennas and Propagation, Vol. AP-9, pp. 506-514, November, 1961.

2) Chen, C.C., "Transmission Through a Conducting Screen Perforated Periodically with Apertures", IEEE Transactions on Microwave Theory and Techniques, Vol. MTT-18, No. 9, pp. 627-632, September 1970.

3) Ott, R.H., Kouyoumjian, R.G., and Peters, L., "Scattering by a Two-Dimensional Periodic Array of Narrow Plates", Radio Science, Vol. 2 (New Series), No. 11, pp. 1347-1359, November 1967.

4) Twersky, V., "Multiple Scattering of Waves and Optical Phenomena", Journal of the Optical Society of America, Vol. 52, No. 2, pp. 145-171, February 1962.

5) Mittra, R., "Relative Convergence of the Solution of a Doubly Infinite Set of Equations", Journal of Research of the National Bureau of Standards - - D. Radio Propagation, Vol. 67D, No. 2, pp. 245-254, March-April 1963.

6) Lee, S.W., Jones, W.R., and Campbell, J.J., "Convergence of Numerical Solutions of Iris-Type Discontinuity Problems", IEEE Transactions on Microwave Theory and Techniques, Vol. MTT-19, No. 6, pp. 528-536, June 1971.

7) Borgiotti, G.V., "Modal Analysis of Periodic Planar Phased Arrays of Apertures", Proceedings of the IEEE, Vol. 56, No. 11, pp. 1881-1892, November 1968.

8) Dufort, E.C., "Finite Scattering Matrix for an Infinite Array", Radio Science, Vol. 2 (New Series), pp. 19-27, January 1967.

9) Altschuler, H.M., and Goldstone, L.O., "A Class of Alternate Modal Representations for Uniform Waveguide Regions", Air Force Cambridge Research Center, AFCRC-TN-57-368, Contract No. AF-19(604)-2031, Report No. R-557-57, February 1957.